Transportation Research Part E 193 (2025) 103857

Contents lists available at ScienceDirect

Transportation Research Part E

journal homepage: www.elsevier.com/locate/tre

Data-driven resilience analysis of the global container shipping network against two cascading failures

Yuhao Cao [a], Xuri Xin [a,*], Pisit Jarumaneeroj [b], Huanhuan Li [a], Yinwei Feng [c], Jin Wang [a], Xinjian Wang [c], Robyn Pyne [a], Zaili Yang [a,*]

[a] Liverpool Logistics, Offshore and Marine (LOOM) Research Institute, Liverpool John Moores University, Liverpool L3 3AF, United Kingdom
[b] Department of Industrial Engineering, Chulalongkorn University, Bangkok 10330, Thailand
[c] Navigation College, Dalian Maritime University, Dalian 116026, PR China

ARTICLE INFO

Keywords:
Maritime Transport
Global Container Shipping Network
Resilience Analysis
Cascading Failures
Redistribution Rule

ABSTRACT

Being a fundamental link in the global supply chain and logistics system, the global container shipping network (GCSN) is highly interconnected, which causes the network resilience challenges by the cascading failures triggered by extreme events (e.g., COVID-19 and regional conflicts). Within this dynamic process, the load redistribution behaviour is the core countermeasure for the propagation of cascading failures, however the diversified mechanism has not been systematically studied. To fill in these gaps, this study aims to develop a pioneering resilience analysis framework against cascading failures, to comprehensively explore the impact of port disruptions on the shipping network resilience. By pioneering the influence analysis of port betweenness, weight, and connectivity on load determination and target selection, a port importance assessment method is applied as the foundation for load redistribution decisions. Based on the global service routes data from 2020 to 2023, the GCSN resilience against the sequential cascading failures of 686 ports worldwide is quantified by three metrics. A scenario analysis is conducted to simulate the effects of cascading failures triggered by 5 historical port disruption events (e.g., the COVID-19 port lockdowns and the 2024 bridge collision at Baltimore port) on resilience of the network. Determining the identified critical capacity threshold is pivotal for effectively enhancing the system's resilience and preventing the likelihood of cascading failures. Additionally, this study offers cutting-edge perspectives to the global shipping industry stakeholders. It presents distinct strategies and preferences, offering actionable advice for port authorities in their risk response decisions. Moreover, this study delivers an economic rationale and critical evaluations, instrumental for the strategic maintenance, planning and augmentation of port infrastructures to prevent unforeseen risks.

1. Introduction

The resilience of transportation systems is conceptualized as a system's ability to accommodate variable and unexpected disruptions (Feng et al., 2024b; Zhou et al., 2019b). A complete process of the changes of resilience usually involves four stages, as shown in Fig. 1, i.e., an equilibrium before the occurrence of a disruption, a response after the disruption, a recovery after the disruption and a

* Corresponding authors.
E-mail addresses: X.Xin@ljmu.ac.uk (X. Xin), Z.Yang@ljmu.ac.uk (Z. Yang).

https://doi.org/10.1016/j.tre.2024.103857
Received 7 March 2024; Received in revised form 27 October 2024; Accepted 5 November 2024

new stability after the recovery (Gu and Liu, 2023).

In shipping networks, disruptions occur from time to time (Feng et al., 2024a). Such disruptions can refer to congestion at ports, accidents at waterways, extreme weather conditions at sea, etc. Analysing resilience can aid in the design and construction of infrastructure and provide a theoretical basis for stakeholders to manage these unforeseen risks (Dui et al., 2021; Hosseini et al., 2019; Qin et al., 2023). Particularly, as the cornerstone of international supply chains, the global container shipping network (GCSN) significantly contributes to the standardized transport of bulk goods (Lee and Song, 2017). As reported by (UNCTAD, 2023), the year 2023 witnessed the trade of approximately 870 million 20-foot equivalent units (TEUs), accounting for about 15 % of the total shipping trade. With its rapid expansion, the GCSN is becoming highly interconnected and complex, amplifying the need for enhanced network resilience. Once disruptions occur at ports and waterways (e.g. natural disasters, geopolitical conflict events, and pandemics), the consequences will cascade outward along these densely connected links, akin to ocean waves (Gadhia et al., 2011). Notable illustrative examples include the Suez Canal blockage (Fan et al., 2022b), the port lockdowns during the COVID-19 pandemic and the Baltimore bridge collision. During the COVID-19 pandemic period, due to anti-epidemic policies, many ports around the world were affected with reduced operational efficiency, leading to decreased resilience in the GCSN. In May 2021, the Yantian port witnessed a significant reduction in capacity, which precipitated considerable cargo delays (Bai et al., 2023). To mitigate these delays, shipping companies had to reroute vessels to alternative ports like Guangzhou and Hong Kong, which in turn caused new congestion at these alternatives. This congestion continued to have a ripple effect, impacting ports in the neighbouring countries and even extending to those in the European and American regions (Xu et al., 2022). This series of chain reactions is called cascading failures. Therefore, as the GCSN grows in complexity and connectivity, the disruption caused by cascading failures on network resilience has become a key challenge in ensuring transportation stability and efficiency.

Currently, the resilience analysis of the shipping network predominantly evaluates one or several static properties, such as topology (Kang et al., 2022; Tsiotas and Polyzos, 2018), modularity (Xu et al., 2020), connectivity (Fan et al., 2022a; Liu et al., 2022a), robustness (Calatayud et al., 2017; Peng et al., 2018; Wang et al., 2016) and vulnerability (Liu et al., 2018; Wu et al., 2019). Dissecting such properties during resilience changes in Fig. 1 offers an intuitive understanding from a practical perspective. Specifically, before any major disruptions occur, shipping networks generally continue to operate at a consistent level. Although shipping networks may encounter minor perturbations, such as temporary congestion or delays, their inherent reliability ensures they can maintain normal operations under such conditions (Gu et al., 2020). However, in the face of major disruptions like natural disasters, port closures, or human interference, the performance of these networks typically begins to decline. Following such events, performance continues to deteriorate, reaching its lowest level. Therefore, during the response stage, the concept of vulnerability denotes the susceptibility of networks to disruptions, where a high vulnerability indicates a rapid loss in performance in the face of disruptions or failures (Gu et al., 2020; Jiang et al., 2024). Robustness, on the other hand, measures the capacity to withstand disruptions, reflecting the remaining performance or capabilities of the system after such events (Xu et al., 2023). Practically, shipping networks are equipped with extra resources or backup systems to ensure continuity even if parts of the network fail. This safety backup, known as redundancy, is exemplified by ports that maintain a higher cargo handling capacity than their daily average, allowing for some flexibility in managing unexpected events (Gu and Liu, 2023). Furthermore, modern shipping networks have been developed to effectively utilise available resources to adjust and recover from disruptions. Networks with higher resourcefulness can return to the normal level more quickly. Nonetheless, the efficiency and speed of this recovery stage are determined by multiple factors such as economics, emergency decision-making and resource deployment. After going through the response and recovery stages, shipping networks may reach a new equilibrium state. This new equilibrium may be the same as the original level, or it may be different, depending on the adjustment and optimisation of networks.

Each of these aforementioned properties assesses the resilience of shipping networks at one or more levels, and a systematic introduction helps to understand the systemic components of network resilience. Although these approaches have achieved the extraction of static features of the network and the identification of key ports, a practical gap still exists, i.e., overlooking the dynamic consequences of cascading failures. In shipping networks, the propagation of cascading failures typically arises from the redistribution

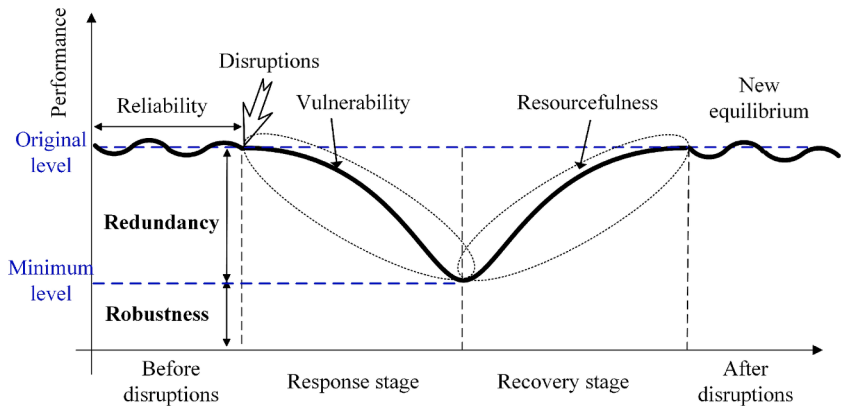

Fig. 1. Four stages of the resilience of shipping networks to disruptions (Gu and Liu, 2023).

of load (i.e., cargo). If a port receives more load than its capacity, it leads to overload or congestion, necessitating the excess load to be redistributed to other ports, thereby resulting in the propagation of cascading failures. Therefore, in this context, the development of an effective resilience analysis framework becomes increasingly vital. Such a framework should be capable of not only modelling the propagation of cascading failures through the GCSN but also providing a comprehensive quantification of the resilience of the entire network. It will make significant contributions to enhancing the risk control capabilities of ports and shipping lines, thereby facilitating a more robust response to similar challenges in the future.

The rest of this study is organized as follows: Section 2 conducts a literature review and identifies current research gaps and corresponding contributions of this study. Section 3 introduces the network modelling, resilience metrics and cascading models in this study. Section 4 illustrates the results regarding the impact of global ports on network resilience and discusses the implications. Section 5 provides the concluding remarks for this study.

2. Literature review

2.1. Resilience analysis of shipping networks

To provide a more explicit view of the state-of-the-art studies, Table 1 develops a detailed examination of representative resilience studies within the context of shipping networks. This review mainly focuses on measurement models and metrics, thereby highlighting the relevant research gaps therein.

A systematic and critical review of current resilience studies in shipping networks reveals several commonalities and key trends. Firstly, typical modelling approaches, such as topological and data-driven models, offer distinct perspectives for understanding and predicting the performance of shipping networks under various challenges. Specifically, topological models, grounded in graph and network theory, are instrumental in deciphering complex shipping systems. They aid in identifying crucial ports and channels within the network, thereby providing a structural understanding of network composition and interconnectivity. Secondly, data-driven models utilize real-world operational data, e.g., liner shipping data (Xu et al., 2022) and automatic identification system (AIS) data (Bai et al., 2023). These models focus on quantitatively assessing changes in network resilience, proving effective in measuring and predicting how the network responds to dynamic operational conditions and disruptions. As a result, benefiting from the advantages of network topology and real data, most studies in Table 1 adopt a combination of both models to quantify network resilience. This hybrid methodology has been validated in terms of its effectiveness in offering a comprehensive understanding of shipping network resilience. Furthermore, when extending the scope of network resilience analysis to a broader transport domain and comparing with studies carried out in road traffic (Duan et al., 2023; Guo et al., 2023), it is evident that shipping network studies, as presented in Table 1, primarily measure changes in network resilience performance in the event of a disruption (Gu and Liu, 2023). In other words, they show limited research scopes in the response state (Fig. 1) without considering the ability for recovery. This distinction arises from the inherent diversity of ports within shipping networks, where the recovery speed is influenced by a multitude of factors, including modellable objective factors and non-modellable human or policy-related factors. This differs from road traffic scenarios where nodes (junctions or stations) and connections (roads or routes) in a given area are typically standardized uniformly (Hosseini et al., 2019). Despite this limitation, recognizing and clarifying this issue also serves to validate the overall direction of the current studies. That is, examining alterations in network resilience resulting from disruptions provides valuable insights, although there remains a space for incorporating a more comprehensive analysis that includes recovery processes.

2.2. Cascading failures

Cascading failures are a common interaction behaviour observed in complex systems, often manifested as continuous and dynamic state changes (Crucitti et al., 2004; Fu et al., 2020; Tang et al., 2016b). In transport systems, cascading failures typically result from dynamic load redistribution involving the transfer of cargoes or passengers and are constrained by the capacity of the hubs (i.e., stations or ports). Therefore, one common approach to model such failures is the Motter-Lai model, also known as the load-capacity model (Motter and Lai, 2002). This model redistributes the load proportionally to the targets and has demonstrated its feasibility through a wide range of applications in the transport and logistics sectors. For example, Tang et al. (2016a) applied it to a two-layer supply chain network. Cumelles et al. (2021) adopted this model to simulate cascading failures within an air network, where the redistributed traffic flow was proportional to the weight of the neighbouring airports. Liu et al. (2022b) employed both the load-capacity and the percolation models to study railway networks, similarly considering the correlation between the redistributed load and the weight of targeted stations. From these studies, it becomes evident that the initiation of cascading failures within networks often results from extreme disruptions (Wang and Chen, 2008). Subsequently, the load redistribution rules define the dynamic changes in the load, leading to hubs constantly failing or overloading (Dou et al., 2010; Wu et al., 2008).

In this context, the selection of targets and the determination of redistributed load have been recognized as pivotal aspects in studying the patterns of the cascading process. Further contributions to redistribution rules have been made in more studies. An attempt in road traffic was made by Qian et al. (2015) to initiate the simulation of road traffic network failures by randomly selecting initial failed nodes and redistributing load based on capacity. Further, Xu et al. (2022) considered two redistribution methods in a shipping network, involving port skipping or selecting alternative ports, and redistributed the load equally to the target ports. This study also pointed out that, different from the accessibility of road traffic, redistribution in the shipping networks also had to consider distance or time constraints. Selecting ports that are too distant can be impractical due to significantly increased economic costs. Following that, Bai et al. (2023) further defined a redistribution rule based on time constraints and port categorisation, with the

Table 1
The resilience metrics and measurement approaches in the studies of the resilience analysis of shipping networks.

References	Resilience metrics	Measurement approaches
(Fan et al., 2022a)	• Resilience:$R = \frac{N_v \times N_s}{N_c}$ where N_v is the connectivity of the network, N_s indicates the size of the network, and N_c denotes the centrality of the network.	Simulation model
(Liu et al., 2023)	• Degree-based resilience:$R_d = \frac{\sum_{j\notin A}^{N} \frac{C_d(j)_{after}}{C_d(j)_{before}}}{N-\lvert A\rvert}$ • Closeness-based resilience:$R_c = \frac{\sum_{j\notin A}^{N} \frac{C_c(j)_{after}}{C_c(j)_{before}}}{N-\lvert A\rvert}$ where A is the set of disrupted ports. $C_d(j)$ and $C_c(j)$ are the degree centrality and closeness centrality, respectively. N represents the set of ports.	Data-driven model
(Xu et al., 2023)	• Structural robustness:$R = \frac{\sum_{Q=1}^{N} S(Q)}{N}$ where $S(Q)$ is the size of the giant connected component (GCC) after removing the Q most important ports, and N indicates the number of ports.	Topological and data-driven model
(Bai et al., 2023)	• Efficiency (the mean inverse shortest travel time):$E = \frac{1}{N(N-1)} \sum \frac{1}{t(i,j)}$Where $t(i,j)$ is the travelling time from port i to port j and N is the number of ports. • GCC • Avalanche size, i.e., the number of failed ports during the cascading process.	Topological and data-driven model
(Baroud et al., 2014a) (Baroud et al., 2014b) (Baroud et al., 2015)	• Resilience*:$R_\varphi(t\lvert e^j) = \frac{\varphi(t\lvert e^j) - \varphi(t_d\lvert e^j)}{\varphi(t_0) - \varphi(t_d\lvert e^j)}$ where $\varphi(t\lvert e^j)$ is the service function at time t with a disruption e^j. t denotes the time in the system recovery phase, t_d indicates the time where system represents disrupted and t_o is the beginning time. *Please note: Various improvements based on this formula were made in these three studies, but only the original formula is showed here to illustrate the underlying principles.	Probabilistic and data-driven model Optimization and data-driven model Data-driven model
(Hossain et al., 2019)	• Vulnerability (absorptive capacity) Weighted mean function:$WMEAN = \sum_i w_i X_i$ where w_i is the weight of the event X_i, $X_i \in \{0,1\}$. • Recoverability (adaptive and restorative capacity) NoisyOR function: $NoisyOR = \begin{cases} 70\%, Adaptivecapacityisachieved \\ 95\%, Restorativecapacityisachieved \end{cases}$	Probabilistic model
(Dui et al., 2021)	• Residual resilience:$R(t) = \frac{Lost(t) - Recovery(t)}{Lost(t)}$ where $Lost(t)$ is the accumulated performance loss during time period t, $Recovery(t)$ denotes the accumulated performance recovery during time period t.	Optimization and simulation model
(Qin et al., 2023)	• Structural resilience:$S_i = \sum_{j\in N} w_{ij}$ Where w_{ij} indicates the weight of the link between port i and port j, N is the set of ports. • Functional resilience:$F_i = \frac{1}{\lambda} \sum_j A_{ij} x_{ij}$ where x_{ij} represents the transportability of node i, λ is a constant, and A_{ij} is the adjacency matrix. • Location resilience:$L_i = \frac{n-1}{\sum_j d_{ij}}$ where d_{ij} denotes the shortest path between nodes i and j, n is the number of ports. • Comprehensive resilience:$R_i = \sqrt{0.34S_i + 0.37F_i + 0.29L_i}$	Data-driven model
(Viljoen and Joubert, 2016)	• Link betweenness • Link salience:$S = \frac{1}{N} \sum_r T(r)$ Where r represents one port in the network, $T(r)$ denotes the sum of the shortest path length from port r to all other ports, and N is the number of ports.	Topological and data-driven mode
(Calatayud et al., 2017)	• Total degree • Betweenness centrality • Average clustering coefficient • Beta index: the average degree of each node • Gamma index: the ratio of the actual number of links to the maximum number • Diameter: the maximum value of the shortest path length among the network	Topological and data-driven model
(Liu et al., 2018)	• Global efficiency:$E = \frac{\sum \frac{1}{l_{ij}}}{N(N-1)}$ Where l_{ij} indicates the shortest path length between node i and j, and N is the number of ports. • Local efficiency: clustering coefficient	Topological and data-driven model
(Wu et al., 2019)	• Connectivity Average degree Isolated-node proportion Clustering coefficient Average shortest path length	Topological and data-driven model

(*continued on next page*)

Table 1 (*continued*)

References	Resilience metrics	Measurement approaches
(Xu et al., 2022)	• Transportation capacity and time Prosperity degree: the sum of weights of all the links. Average shortest shipping time • Dependence Dependence degree: the total weights of the ports in a given area before and after the disruption of the main channel. • Unweighted efficiency:$E = \frac{1}{N(N-1)}\sum\frac{1}{d(i,j)}$ Where $d(i,j)$ is the shortest path length between port i and port j, N is the number of ports. • Weighted efficiency:$WE = \frac{1}{N(N-1)}\sum\frac{l(i,j)}{dis(i,j)}$ where $dis(i,j)$ is the shortest sailing distance between port i and port j, $l(i,j)$ indicates the geographical distance between port i and port j.	Topological and data-driven model

redistributed load being proportional to the total traffic flow through the target ports. As research progresses, two additional studies refined the redistribution rules at the overall and individual levels, respectively. Duan et al. (2023) applied the load-capacity model with an innovative consideration of the independent and collective behaviour of users, effectively framing it as an overall optimisation problem between user equilibrium (UE) and system optimum (SO). While at the individual level, Guo et al. (2023) expanded upon this model by incorporating differences in the redistribution of larger and closer stations. Specifically, the proportion of redistributed load was determined by a combination of the residual capacity and the betweenness centrality (BC) of the neighbouring stations, which is a reflection that inspires us to further explore more factors affecting redistribution.

2.3. Research gaps and contributions of this study

From the aforementioned literature, it is evident that progress has been made in assessing resilience and modelling cascading failures. Combined with the need for realistic development of the shipping network, this study identifies three key research gaps and proposes corresponding contributions:

Gap 1: A majority of the studies in Table 1 overlook certain characteristics of shipping networks, such as the dynamism and the directed-weighted connectivity. This oversight underscores persistent research gaps in the field. Firstly, due to the interconnectivity of shipping networks, disruptions that occur at key transport hubs can quickly spread to other ports and/or the port states through port centric logistics systems. While the static topological analysis or quantitative assessments carried out by the previous studies fail to effectively capture the dynamic nature of the network. This gap significantly curtails the practical application of these studies as they could not achieve a valid response to the impact of these disruptions on the industry. Secondly, regarding resilience metrics, the existing metrics often address one of the aspects of the weighted and directed nature of shipping networks in calculations. For example, although the concept of weighted efficiency (WE) has been proposed (e.g., in the network disintegration model or the distance weighted efficiency), these metrics are often calculated under the assumption of an undirected network, which is not rigorous in network theory (Wang and Chen, 2008). Thirdly, in the context of network cascade failures, successive failures or overloads challenge the safety operation of ports. Maintaining a certain level of security redundancy is now a common practice in dealing with unknown risks and disruptions. The dynamic variations of network redundancy can effectively reflect the resilience changes and indicate the adequacy of such safety backups in the network, but the relevant measurement metric is still missing.

Contribution 1: This study employs attributes-based metrics, namely robustness and redundancy, to explicitly measure the dynamic changes in the network resilience due to cascading failures. Modelling the GCSN as a weighted and directed network, the giant weakly connected component (GWCC) and the network disintegration model are innovatively adapted to systematically assess the robustness in terms of the directed connectivity and weighted efficiency. Additionally, utilizing the global container shipping data from 2020 to 2023, a new metric called the redundancy ratio (RR) is proposed to capture the characteristics of the network in terms of its capacity backup (i.e., safety redundancy). This metric provides an economic justification and valuable insights for port operation and construction to prevent unknown risks.

Gap 2: The cascading failure in a transport system is typically triggered by the redistribution of loads. In studies of shipping networks, common practices involve the proportional redistribution of the load from a failed port across multiple ports. This is effective for the failure of a large port where the load is substantial and challenging to transfer via a single vessel or be accommodated by a single port. This necessitates the engagement of multiple vessels and multiple ports. However, in practical scenarios, there exists a significant disparity in load between large and small ports. Small ports often prefer to transfer cargo directly to their neighbouring mega ports to avoid additional costs, such as berthing fees. Thus, such diversified redistribution in shipping networks is still missing. The practicality of single-target redistribution and multi-target redistribution, as well as their comparative analysis, remain an unexplored area.

Contribution 2: This study pioneers two novel redistribution rules for modelling cascading failures: the breadth first redistribution rule (BFRR) and the depth first redistribution rule (DFRR). The BFRR facilitates fast response and broad load propagation, effectively capturing the essence of multi-target load transfers. In contrast, the DFRR concentrates on single-target redistribution, highlighting the profound effects that disruptions can have on a specific port within the network. These two redistribution rules represent distinct strategies and preferences, providing practical insights for the port risk management and response decisions.

Gap 3: For both single-target and multi-target redistribution, determining the redistributed targets and the proportion of redistributed load remains challenging. Previous studies have attempted to use criteria such as capacity (Bai et al., 2023; Cumelles et al., 2021), degree, BC (Guo et al., 2023) or average redistribution (Xu et al., 2022) as the basis to simulate this dynamic redistribution process. That is, the proportion of load redistributed to the different target ports is determined by the proportion of a single parameter value (e.g., capacity, degree or BC) at the target port, or is redistributed equally to each port. However, making decisions based on a single criterion is neither comprehensive nor practical. Drawing inspiration from the study of (Guo et al., 2023), which suggested a more practical approach to choosing targets between larger and closer stations. Similarly, in the practice of the shipping industry, whether it is multi-target or single-target redistribution, the considerations of port managers when choosing redistribution targets and determining proportions also include multiple factors, such as cargo handling capacity and transshipment capacity. These factors can

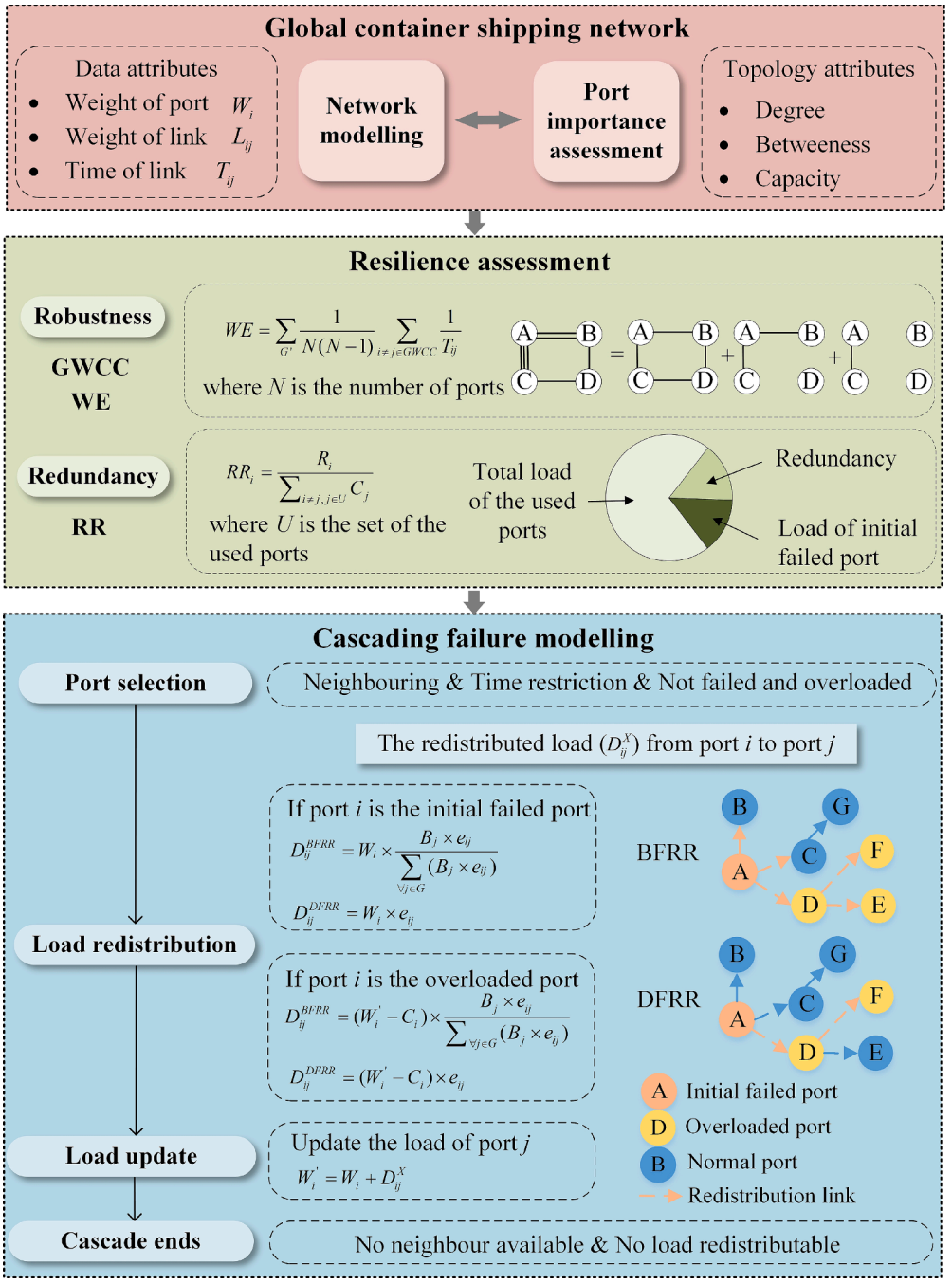

Fig. 2. The methodological framework.

be represented in network theory as parameters such as node weight, degree and BC. Consequently, there is a gap in the literature regarding a holistic approach that can incorporate these multifaceted considerations in an integrated manner.

Contribution 3: By considering both port topology and flow holistically, the proposed rules facilitate load redistribution by prioritizing ports through a comprehensive assessment of their importance. The Borda count method ranks ports according to attributes, which are aggregated by evaluating 627 ports globally. This minimizes the influence of individual specificities and ensures a more balanced and objective process for determing redistribution targets and managing loads during cascading failures.

3. Methodology

This section outlines the methodology through three interconnected aspects: 1) the GCSN modelling, 2) the definition of the resilience metrics and 3) the models of cascading failures. The framework flowchart is demonstrated in Fig. 2, and Table 2 lists the notations and acronyms.

3.1. Global container shipping network modelling

The data used in this study is the service routes data, collected from a leading database in global vessel and schedule tracking, namely BlueWater Reporting Application Server (www.bluewaterreporting.com). The database is launched by ComPair Data, Inc., which totally covers 2607 liner service routes from 298 ocean carriers, providing the most comprehensive liner services database available today (www.compairdata.com). Different with the vessel trajectory data, which contains voyage logs, the service data schedules and records the port rotation activities of a complete service route (Xu et al., 2020). The raw data in this study provides information on each service route, including the order of calling ports, the deployed cargo service capacity (unit: TEUs), the service frequency, the sailing time between two consecutively called ports and the basic properties of vessels sailing on this route (Jarumaneeroj et al., 2023). Therefore, to ensure the state of the art and the breadth of the research scope, this study accesses the global service routes data from 2020 to the second quarter of 2023 (this is the latest data available at the start of this study), covering 686 ports worldwide.

In this study, the network theory is used to establish the GCSN, denoted as G. Modelling ports within service routes as nodes, a link e_{ij} exists between two nodes (e.g., port i and port j) if they are consecutive calling ports on a service route (Bai et al., 2023). Therefore, $e_{ij} = 1$ denotes that port i and port j are directly connected in G and such port-to-port link may exist in multiple service routes. By identifying and integrating all port-to-port links, this study aggregates the raw data so that each record in the port-to-port link data consists of: origin, destination, number of services containing this port-to-port link, number of vessels participating in this link, average traffic weight on this link (unit: TEUs/week), and average sailing time on this link (unit: days). Therefore, a directed weighted GCSN with 686 nodes and 6064 links is established in this study, where the weight of a given link is the sum of the capacity of all container ships sailing through the link. By identifying all links from port i to other ports, the weight of port i is defined as $W_i = \sum_{\forall j \in G, i \neq j} L_{ij}$, where L_{ij} denotes the weight of the directed link $(i.j)$. The established network is illustrated in Fig. 3. Following the Motter-Lai model (Motter and Lai, 2002), the capacity of port i is proportional to its weight, as defined in Equation (1):

$$C_i = \lambda \times W_i \tag{1}$$

Table 2
The notation and acronym list.

Notation	Definition
GCSN	Global Container Shipping Network
GWCC	Giant Weakly Connected Component
WE	Weighted Efficiency
R	Redundancy
RR	Redundancy Ratio, RR_i denotes the network redundancy ratio after propagating cascading failures triggered by the initial failed port i
BFRR	Breadth First Redistribution Rule
DFRR	Depth First Redistribution Rule
BC	Betweenness Centrality
G	The GCSN model
W_i	The weight of port i
C_i	The capacity of port i
λ	The capacity multiplier,$\lambda \geq 1$
N	The number of ports in the GCSN
e_{ij}	The index of a directed link existing between port i and port j
L_{ij}	The weight of directed link e_{ij}
T_{ij}	The sailing time from port i to port j
U	The set of the used ports
B_i	The Borda score of port i
D	The redistributed load, D_i denotes the redistributed load from port i, D_{ij}^X denotes the redistributed load from port i to port j according to the rule X, where $X = \{BFRR, DFRR\}$.
P_{ij}	The proportion of the redistributed load from port i to port j

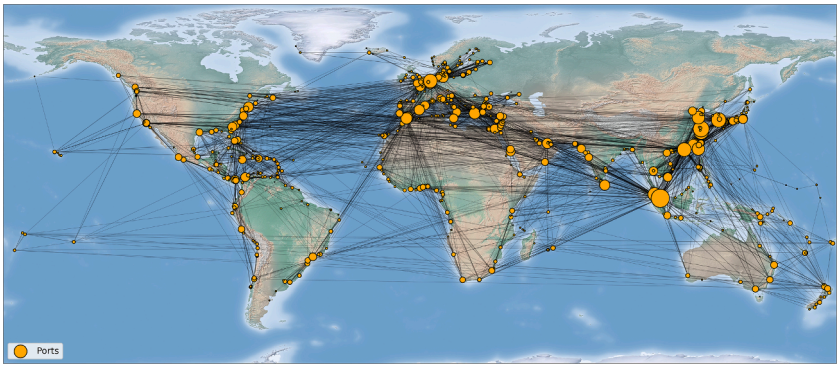

Fig. 3. The established Global Container Shipping Network.

where λ ($\lambda \geq 1$) denotes the capacity multiplier.

3.2. Resilience metrics

In this section, two topological metrics (i.e., GWCC and WE) and an economic rationale (i.e., RR) are proposed to systematically assess the resilience of the GCSN in terms of robustness and redundancy.

3.2.1. Robustness metrics

Based on the review in Section 2.1, it can be known that some studies have applied the giant connected component (GCC) to assess network connectivity after disruptions (Xu et al., 2022). Generally speaking, in an undirected network, a connected component is a subgraph which contains at least two nodes connected by an edge. Within a large scale network, the network may suffer from disruptions in one or more nodes, subsequently causing the loss of functionality. These failed nodes are considered to be removed from the network and disconnection from other nodes. As a result, the entire network may be divided into several separate subgraphs. In that case, the subgraph with the most nodes serves as the GCC and the number of nodes represents the size of the GCC (Dorogovtsev et al., 2001; Newman et al., 2001).

Although the GCC is capable of measuring the connectivity of the network, its application is limited to undirected networks. Therefore, two analogous concepts named the Giant Weakly Connected Component (GWCC) and Giant Strongly Connected Component (GSCC) are typically utilized in the directed networks (Dorogovtsev et al., 2001). Specifically, in a directed graph, the GWCC is the largest subgraph where any two nodes are connected by a link if the direction is ignored. In other words, when considering links as undirected, it forms a GCC. While in a directed graph, the GSCC is the largest subgraph where any two nodes are connected by links that respect the direction of the links. This means that the link from any node to any other node within this subgraph must be bidirectional (Liu et al., 2017). Theoretically, the GSCC has a stricter prerequisite assumption than the GWCC, i.e., nodes in the GSCC must all be bi-directionally connected, whereas nodes in the GWCC only need to be connected. Practically, the existence of a link from port A to port B does not necessarily mean that there will be a link from port B to port A. Also, the primary concern in this study is whether there is any possible link between ports to ensure connectivity for logistical planning. Therefore, in practical scenarios, the GWCC tends to be larger and includes more ports, offering a broader view of the ability of the network to reroute or reverse direction and how interconnected the network is. In this study, by modelling the GCSN as a directed network, the GWCC is found by the Depth First Search (DFS) algorithm and then the size of the GWCC can be calculated by counting the number of ports within the GWCC.

Furthermore, from the studies of the literature (Zhou et al., 2021; Zhou et al., 2019a), another robustness metric is efficiency. In network science, efficiency measures the effect of network structure on information or resources transfer (Sørensen et al., 2012). Applied to shipping networks, this is reflected in the sailing distances between ports. High efficiency could be represented by a shipping network with densely distributed ports, enabling efficient cargo transport. Thus, a common way to calculate efficiency is to calculate the average shortest sailing distance between any two ports in a network. This method is valid for measuring the efficiency of an intact network but will fall short in disrupted networks due to immeasurable or infinite distances to isolated nodes. To address this, Latora and Marchiori (2001) introduced an alternative method for calculating efficiency based on the average inverse shortest distance between nodes, as shown in Equation (2):

$$Efficiency = \frac{1}{N(N-1)} \sum_{i \neq j \in G} \frac{1}{d_{ij}} \tag{2}$$

where N denotes the number of nodes in the network G and d_{ij} indicates the shortest distance between node i and node j. This study substitutes distance by sailing time, as it can better intuitively represent connectivity, accounting for various meteorological and geographic factors (Bai et al., 2023).

Additionally, another important attribute in calculating efficiency is the consideration of load on links, which refers to the weight of links. In practice, disruptions impact routes unevenly. Disruptions on the links with heavier loads will have greater practical impli-

cations compared to links with lighter loads. Therefore, Zhou et al. (2019a) proposed a network disintegration method to assess the impact of weighted links on efficiency. A simple toy model can be seen in Fig. 4. The logic of this model is to use the number of edges to represent the weight of a given link, with one edge representing a standard unit. Subsequently, the entire network undergoes disintegration iterations, where the weights on all links are reduced by one unit at a time, effectively subtracting one edge. The subtracted edges are formed into a new subgraph, which has the same number of nodes as the original network. If the weight of a link is reduced below 0 at an iteration, that link will not be present in the subgraph generated in subsequent iterations. Thus, the weight of any link in each subgraph is one unit. Using the toy model in Fig. 4 as an example, the link between node A and node B has a weight of 2 units, so that link will only appear in the first two subgraphs. After the disintegration is complete, the efficiency of the original network is the sum of the efficiency of all subgraphs. In order to capture the variability between links having different loads while avoiding computational complexity, 1000 TEUs is chosen as the standard unit in this study. The calculation of the WE is outlined in Equation (3):

$$WE = \sum_{G'} \frac{1}{N(N-1)} \sum_{i \neq j \in GWCC} \frac{1}{T_{ij}} \tag{3}$$

where G' denotes the subgraph set after the disintegration and T_{ij} indicates the sailing time from port i to port j. Here, N represents the number of ports within the GCSN, $N = 686$. Therefore, combined with the previously introduced concept, when a disruption occurs at a port within the GCSN, the size of the GWCC and the WE are calculated at the end of the cascading process to measure the remaining connectivity and robustness.

3.2.2. Redundancy metrics

In a shipping network, the capacity of a port generally surpasses its practical load, with the exceeding part termed as "reserve capacity". Therefore, a network equipped with adequate reserve capacity can effectively cope with unforeseen disruptions and risks. This concept of safety backup is also known as redundancy (Murray-tuite, 2006; Sambowo and Hidayatno, 2021). In this study, following a disruption in a network, the load of the initial failed port continuously cascades to more ports, which activates their reserve capacity to accept the redistributed load. If the redistributed load exceeds the reserve capacity, the excess continues to be redistributed to the subsequent ports, until either the initial load is fully absorbed or no ports remain for redistribution. At this point, the sum of the reserve capacity remaining in all used ports (i.e., ports that have been redistributed load) is defined as the redundancy, and the proportion of this reserve capacity to the total capacity is defined as a redundancy ratio. Therefore, assuming the network redundancy after the cascading failures triggered by the initial failed port i is R_i and the redundancy ratio is RR_i, they are calculated as Equations (4) and (5):

$$R_i = \left[(\lambda - 1) \sum\nolimits_{i \neq j, j \in U} W_j \right] - W_i \tag{4}$$

$$RR_i = \frac{R_i}{\sum_{i \neq j, j \in U} C_j} \tag{5}$$

where U represents the set of the used ports. $\left[(\lambda - 1) \sum_{i \neq j, j \in U} W_j \right]$ is the reserve capacity of the used ports.

By calculating the network redundancy, the ability of the GCSN to cope with disruptions in different ports can be effectively reflected and quantified in an economic term (i.e., cargo units). A large RR indicates that the ports that are theoretically reachable from the initial failed port have sufficient safety backup capacity to cope with the cascading failures effectively. However, a negative redundancy indicates the inability to absorb the load from the initial failed port, leading to potential economic losses. It is important to note that redundancy calculation focuses on used ports, not the entire network. This is because, for unused ports, two scenarios can occur: 1) the load of the initial failed port has already been consumed and the participation of the remaining ports is not required, and 2) the remaining ports are isolated outside the GWCC due to the propagation of the cascading failures, which in practice represents the inaccessibility. Therefore, the inclusion of these inaccessible ports or the ports that will not participate is not practical. The RR should be evaluated alongside the GWCC size and the WE. A scenario characterized by both a smaller size and a smaller WE, coupled with a smaller RR, implies that the network is nearing complete overloading or failure due to cascading failures. This could lead to substantial congestion and delays, as the load from the initial failed port overwhelms most of the network.

3.3. Cascading failure modelling

Based on the established GCSN, a key to achieve a dynamic assessment of network resilience is the modelling of cascading failure propagation. As mentioned in Section 2.2, cascading failures start with the disruption of a port in the network, which in turn

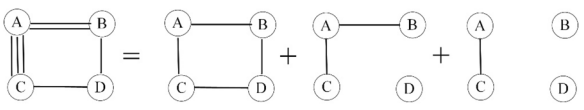

Fig. 4. The toy model of the network disintegration method (Zhou et al., 2019a).

redistributes the load from the failed port to other ports. In this section, a comprehensive port importance assessment is defined to determine the redistributed targets and load. Then, two redistribution rules, i.e., the BFRR and the DFRR, are proposed to model the different propagation preferences.

3.3.1. Port importance assessment

The importance of a port provides a comprehensive response to its role in the network. In this study, the importance of a port determines the proportion of redistributed load in the BFRR and the redistributed targets in the DFRR, respectively. In practice, the importance of a port needs to be assessed in terms of its role in various aspects, including scale (weight), betweenness, and connectivity. These properties are reflected in complex network theory as weight, BC and degree. Specifically, a port with a higher weight indicates greater cargo handling ability; a port with a larger BC is located in a more critical bridge position, facilitating the transfer of cargo between different ports; and a port with a higher degree has higher connectivity, which enables the transhipment of cargo to a larger number of ports. Therefore, to integrate these properties for a holistic assessment, with reference to the literature (Liu et al., 2018), the Borda count method is applied to identify the importance of each port within the GCSN.

The Borda count method is a scoring method for voting and ranking decisions. In this study, the ports within the GCSN are candidates and the properties are the voters. For any port, the score for each property depends on its ranking within the GCSN. For example, among all 686 ports, if port i ranks first in weight, it receives a score of 686; if it ranks second in BC, it receives a score of 685; and if it ranks third in degree, it receives a score of 684. Therefore, the total Borda score B_i for port i is 2055 (i.e., $686 + 685 + 684 = 2055$). In cases where ports share the same rank (e.g., two ports both ranking first in degree), they receive an average score (in this case, 685.5 each).

This method effectively manages scenarios with multiple criteria, sidestepping the complexities and subjective biases inherent in assigning arbitrary weights to different factors (Alipour et al., 2014). In this study, the main purpose of conducting the comprehensive assessment is to develop subsequent redistribution rules through a composite indicator that integrates multiple properties of a port. Sometimes, other studies may want to further explore the relative importance between these properties, and then it is often necessary to introduce some parametric methodological approach, but this is not the focus of interest in this study.

3.3.2. Two redistribution rules

It has been mentioned previously that there are two redistribution rules in the cascading failures propagation, inspired by the breadth-first search algorithm and the depth-first search algorithm, in turn named as the BFRR and the DFRR. In this study, to enable a clear description of the two types of redistribution rules, four possible states of the ports within the GCSN are shown in Table 3. In addition, the states “Initial failed” and “Overloaded” are mutually exclusive with other states.

Therefore, the redistribution rules contain the following steps, and a flowchart of the cascading process is shown in Fig. 5.

1) Iteration of all ports as initial failed ports

The cascading failure starts with an unexpected disruption of a port in a network. In this study, all ports iterate this process once as the initial failed port. In each iteration, the load from the initial failed port is first redistributed within the network, and the redistributed targets update their states after receiving the load. The redistribution process continues until either no new overloaded port emerges (i.e., the load of the initial failed port has been absorbed by the network) or until the network itself collapses.

2) Selection of the redistribution targets

For both the BFRR and the DFRR, the redistributed targets need to satisfy the following conditions:

- Neighbouring. The redistributed targets should be the neighbour ports of the initial failed port or the overloaded ports, i.e., for $\forall i, j \in G$, $e_{ij} = 1$. Notably, since this network is directed, redistributed targets are restricted to the successors directed from the initial failed or overloaded port. This would be consistent with operational realities as the transport of containers from port i to port j is not necessarily bidirectional, and disruptions are likely to impact directly connected ports by such pre-existing service routes.
- Time restriction. This restriction is intended to enhance the practical implications, as selecting ports that are too far away makes operating costs too high and economically unrealistic. Referring to related studies (Bai et al., 2023; Xu et al., 2022), this study also sets the time restriction, i.e., only neighbour ports whose sailing time are less than the average sailing time of the GCSN (i.e., 5 days)

Table 3
Four states of the ports within the GCSN.

State	Clarification
Normal	Ports are not in states of initial failure, overloaded, or used.
Initial failed	Ports that experience initial disruptions rendering them non-functional. Their entire load needs to be redistributed.
Overloaded	Ports where the sum of redistributed load and own load exceeds their capacity, operating in a dynamic equilibrium. Excess load is further redistributed.
Used	Ports that have received redistributed load.

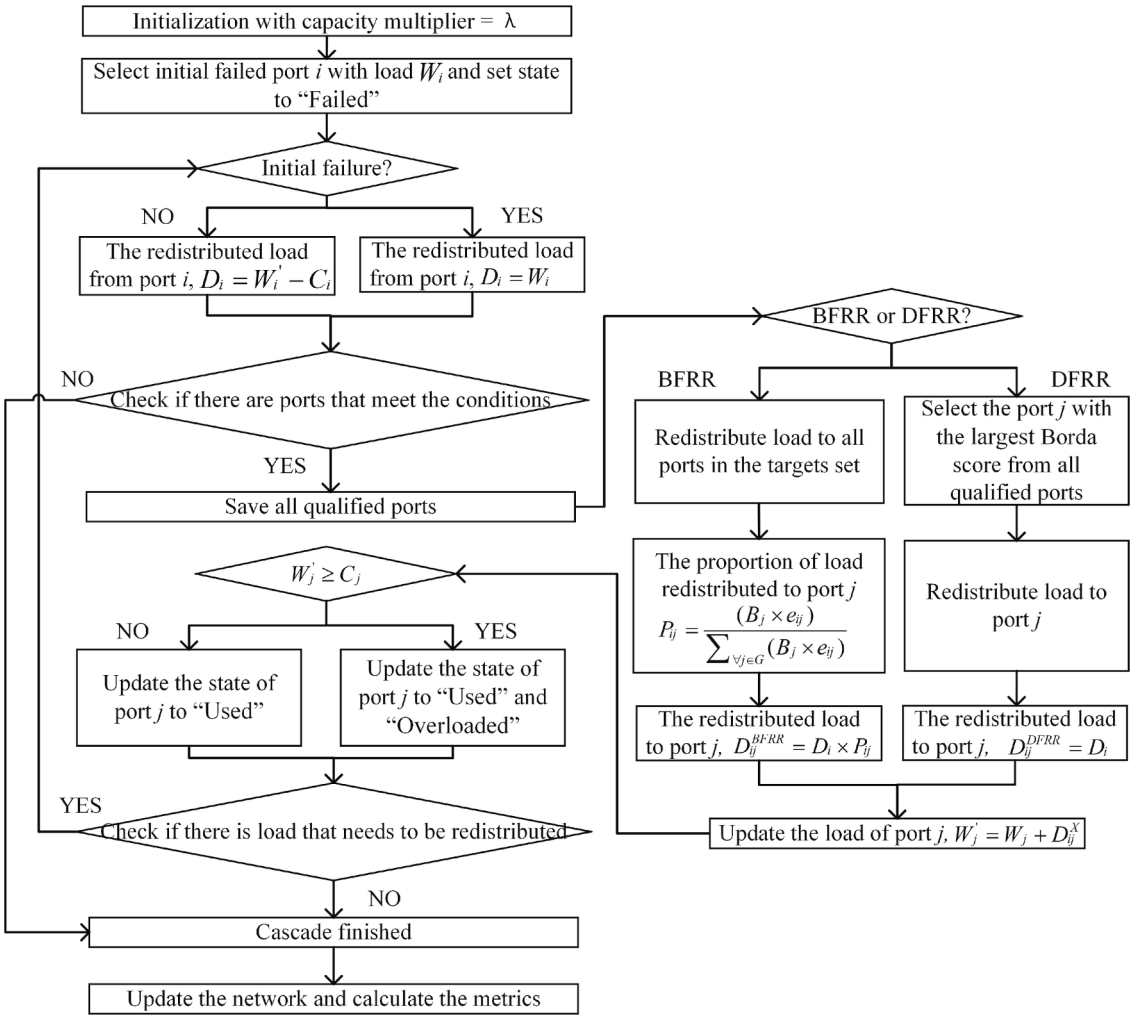

Fig. 5. The flowchart of the cascading process.

are qualified. If no neighbouring port reaches the threshold, this time restriction is increased by 1 day and the selection process is repeated until at least one neighbouring port becomes available.

- Not failed and overloaded. The states of the redistributed targets should be neither initially failed nor overloaded. Although the overloaded ports remain functional and could theoretically be redistributed, i.e., in the dynamic equilibrium mentioned in Table 3, practically, stakeholders generally do not consider selecting overloaded ports for redistribution, as such redistribution would exacerbate congestion and delays, which will highly likely require secondary redistribution and increase costs.

After specifying these three conditions, the BFRR will select all ports that meet all of the conditions to redistribute the load, while the DFRR will select only one target. At this point, based on the prior port importance assessment, the port with the largest Borda score is deemed to possess a superior overall capacity to handle cargo. Therefore, the port with the largest Borda score among ports that satisfies all the conditions will be selected as the target for redistribution in the DFRR.

3) Redistribution of the load

From Table 3, two states of ports need to redistribute load, i.e., the initial failed port and the overloaded ports. The two types of ports redistribute their full load and the load that exceeds the capacity to the targets, i.e., $D_i = \begin{cases} W_i, portiisinitialfailed \\ W_i^{'} - C_i, portiisoverloaded \end{cases}$. For the DFRR, since only one redistribution target is selected at a time, then the all-or-nothing (AON) redistribution is adopted, i.e., all the load is redistributed to the selected port, as shown in Equation (6):

$$D_{ij}^{DFRR} = D_i \times e_{ij} \tag{6}$$

where D_{ij}^{DFRR} represents the redistributed load from port i to port j according to the DFRR, and port j is the port with the largest Borda score among ports that satisfies all three conditions. However, for the BFRR, since multiple targets are selected, the redistribution proportion for each target needs to be decided based on the pre-determined port importance. Here P_{ij} denotes the proportion of the redistributed load from port i to port j according to the BFRR, which is determined by the Borda score B_j, as shown in Equation (7):

$$P_{ij} = \frac{B_j \times e_{ij}}{\sum_{\forall j \in G}(B_j \times e_{ij})} \tag{7}$$

Therefore, in the BFRR, the redistributed load is proportional to the importance of the port, as shown in Equation (8):

$$D_{ij}^{BFRR} = D_i \times P_{ij} \tag{8}$$

where D_{ij}^{BFRR} denotes the redistributed load from port i to port j according to the BFRR. Subsequently, regardless of whether it is based on the BFRR or the DFRR, the load of port j, after receiving the redistributed load from port i, is updated as $W_j' = W_j + D_{ij}^X$, where X denotes the BFRR or the DFRR. If the updated load W_j' of port j exceeds its capacity C_j, the state of port j is updated to "Overloaded", otherwise it is updated to "Used".

4) Removal of the ports and calculation of the metrics

When the redistribution and iteration of the cascading failures are finished, the network removes the ports which have the states of "Initial failed" and "Overloaded", including the ports and their connected links. The resilience metrics are calculated in the remaining network.

4. Results

4.1. Resilience analysis against cascading failures

4.1.1. Port importance ranking

Based on the data and the network modelling proposed in Section 3.1, the established GCSN, containing 686 ports and 6064 links, demonstrates a globally dense regional distribution. As depicted in Fig. 3, ports in East and South Asia show greater weight, and ports in the European region exhibit denser clustering. To specifically explore the importance of ports, the Borda count method described in Section 3.3.1 integrates degree, weight, and BC to globally rank 686 ports in a comprehensive manner, and the top 20 ports are shown in Table 4.

Overall, the top 20 ports comprise most key hubs in the global shipping network with coverage of Asia, Europe and the Americas. Among the global ports, the Port of Singapore ranks first in terms of comprehensive importance, accounting for the first place in terms of degree, weight and BC respectively. This ranking aligns with the real-world prominence of Singapore as a vital hub port. Strategically located at the crossroads of the Pacific and Indian Oceans, remarkable position and transshipment capabilities of Singapore have established it as one of the busiest ports in the world (Xu et al., 2020). An interesting observation from this study is the comparison between the ports of Busan and Shanghai. Despite Shanghai has more pronounced weight advantage, the superior connectivity

Table 4
Top 20 ports ranked by the comprehensive importance assessment.

Port code	Port name	Degree	Weight	BC	Degree score	Weight score	BC score	Borda count	Rank
SGSIN	Singapore	164	1,738,060	0.163	686	686	686	2058	1
KRPUS	Busan	157	1,042,943	0.115	685	683	684	2052	2
CNSHA	Shanghai	133	1,546,715	0.067	683.5	685	682	2050.5	3
NLRTM	Rotterdam	133	703,858	0.120	683.5	678	685	2046.5	4
BEANR	Antwerp	124	559,211	0.080	682	675	683	2040	5
MYPKG	Klang	117	778,229	0.057	681	679	679	2039	6
GRPIR	Piraeus	107	409,521	0.061	677	669	681	2027	7
TWKHH	Kaohsiung	114	631,629	0.033	680	676	670	2026	8
ESALG	Algeciras	110	404,947	0.061	678	667	680	2025	9
MAPTM	Tanger Med	103	465,035	0.050	675.5	672	677	2024.5	10
CNNGB	Ningbo	103	1,308,077	0.026	675.5	684	663	2022.5	11
HKHKG	Hong Kong	112	885,351	0.024	679	682	658	2019	12
CNTAO	Qingdao	99	786,753	0.026	674	680	664	2018	13
MYTPP	Tanjung Pelepas	96	463,864	0.043	673	671	674	2018	14
ESVLC	Valencia	82	381,037	0.040	668	664	671	2003	15
CNYTN	Yantian	72	822,705	0.022	664	681	657	2002	16
AEJEA	Jebel Ali	70	449,936	0.032	662.5	670	668	2000.5	17
DEHAM	Hamburg	86	407,825	0.026	671	668	661	2000	18
USNYC	New York	68	394,786	0.041	660	665	672	1997	19
CNSHK	Shekou	93	672,389	0.015	672	677	648	1997	20

and transit benefits of Busan earn it a higher Borda score. Such a comprehensive approach and analysis result is a success in responding to real-world decision-making processes, which often rely on multifactorial considerations, especially in the context of load propagation.

Having established the Borda scores for all 686 ports on a global scale, a robust basis can be possessed for proceeding with subsequent network resilience analysis steps. These scores play a crucial role in defining the load redistribution proportion under the BFRR and in selecting the appropriate ports for load redistribution under the DFRR. This methodical approach ensures that the network resilience analysis is grounded in a thorough and practical understanding of each port's significance within the global shipping landscape.

4.1.2. *BFRR-based cascade*

The BFRR-based cascade redistributes the load from the failed or overloaded ports to at least one eligible port proportionally. In this study, each of the 686 global ports is iteratively treated as an initial failed port, following which the cascading failure process is simulated. Referring to existing studies (Bai et al., 2023; Cumelles et al., 2021), the capacity multiplier of global ports is set to 1.3, i.e., $\lambda = 1.3$.

For the original GCSN, the size of the GWCC and the WE are 686 and 0.092, respectively. When iterating each port as the initial failed port and applying the BFRR for load redistribution, significant variations are observed in the size of the GWCC, the WE, and the RR across different ports. These variations highlight the impact of each port's failure on the overall resilience of the GCSN. For example, when the Port of Singapore is used as the initial failed port, its load needs to be constantly redistributed based on the BFRR, which in turn triggers the propagation of cascading failures. This process results in a size of GWCC of 649, a WE of 0.0779, and an RR of 0.14, quantifying the extent to which substantial disruptions occurring in the Port of Singapore will cause the network resilience. Therefore, Figs. 6-8, highlight the ports falling within the top 1 % and 5 % of the corresponding cumulative distribution functions (CDF), in terms of the size of GWCC, the WE and the RR, (i.e., the ports with the lowest values of the size of GWCC, the WE and the RR), respectively.

From the perspective of robustness, a more specific statistical information can be shown in Table 5, which lists the seven ports highlighted in yellow in Figs. 6 and 7. These identified ports are mainly located in Asia and Europe, indicating a positive correlation with the development of the local shipping industry and economy. By further examination, all these ports consistently secure positions within the top 20 in terms of importance. This aligns with the practical understanding that failures at more critical ports have a more disruptive effect on network resilience and the global shipping economy. A case in point is the Port of Rotterdam. Its failure leads to 114 ports in the GCSN being redistributed and 66 ports being overloaded, reducing the GWCC size to 614 which is the lowest among all ports. Such a failure scenario at Rotterdam, possibly triggered by extreme events, implies that redistributing its load to other ports under the BFRR would cause significant overloading or blocking of 66 ports. Following that, there are additional 6 ports isolated from the GWCC, which may fail to trade with most of the ports due to the lack of accessible links or transshipment ports. In addition, the WE of the GCSN reduces to 0.0675, less than 75 % of the value in the original network. This can be explained that, due to extensive port closures, it is inaccessible for those overloaded or congested ports within some of the shortest paths, which makes it necessary for vessels to take a detour and raise the sailing time, thus leading to a decrease of network efficiency. Therefore, when considering the impact of failures at ports listed in Table 5, it becomes evident that the GCSN resilience significantly diminishes in each scenario. With a minimum of 20 ports becoming overloaded in each case, these failures could lead to considerable economic losses within the global shipping industry.

From the perspective of redundancy, all seven ports in Table 5 could maintain certain safety redundancy in these scenarios. For

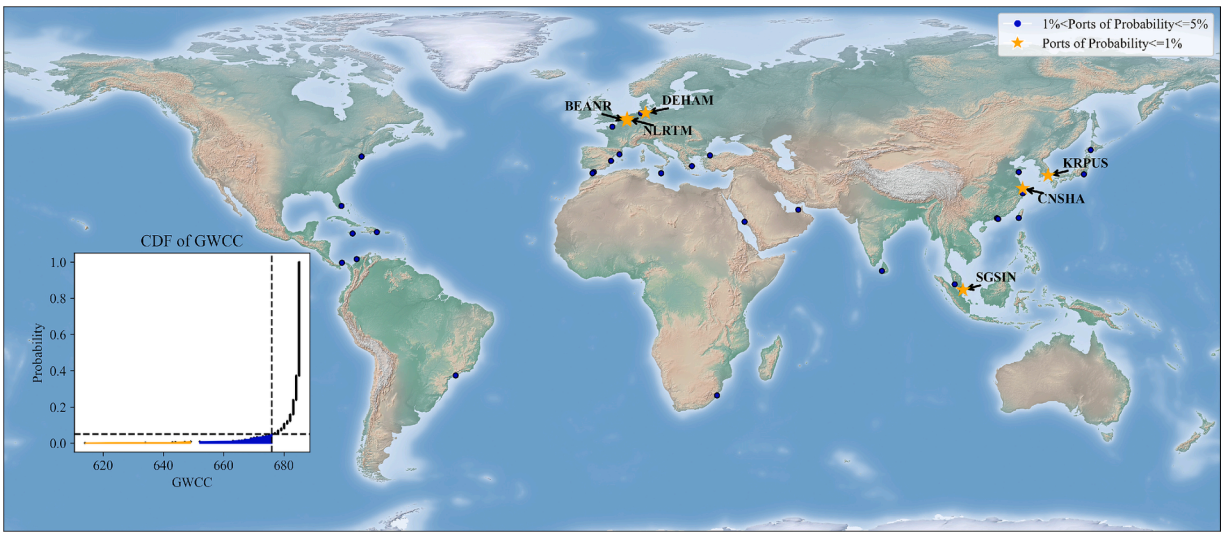

Fig. 6. The distribution of the ports based on the size of the GWCC in the BFRR-based cascade.

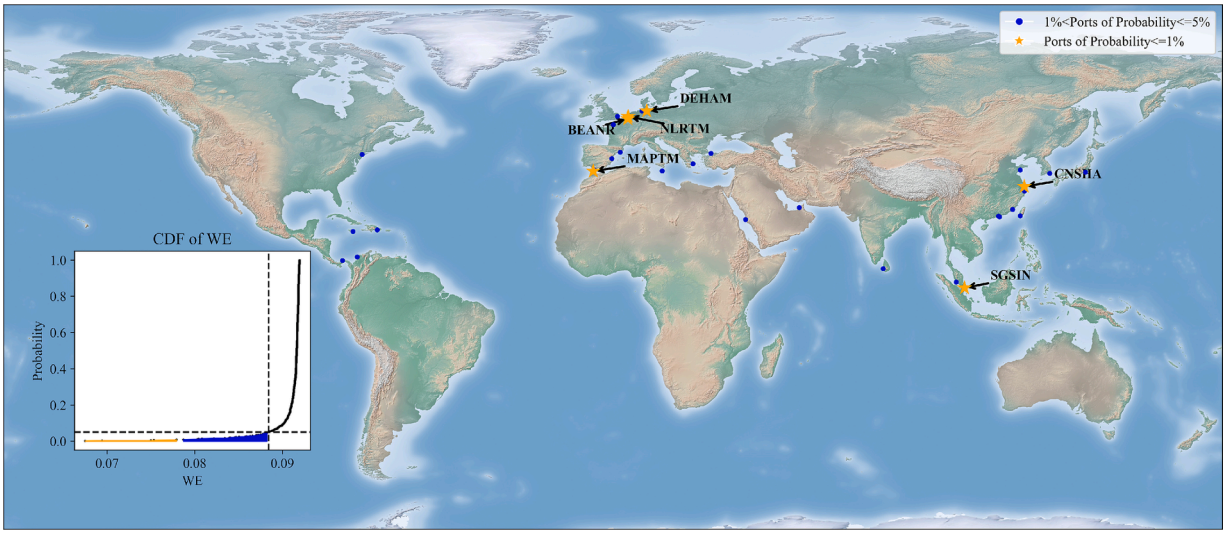

Fig. 7. The distribution of the ports based on the WE in the BFRR-based cascade.

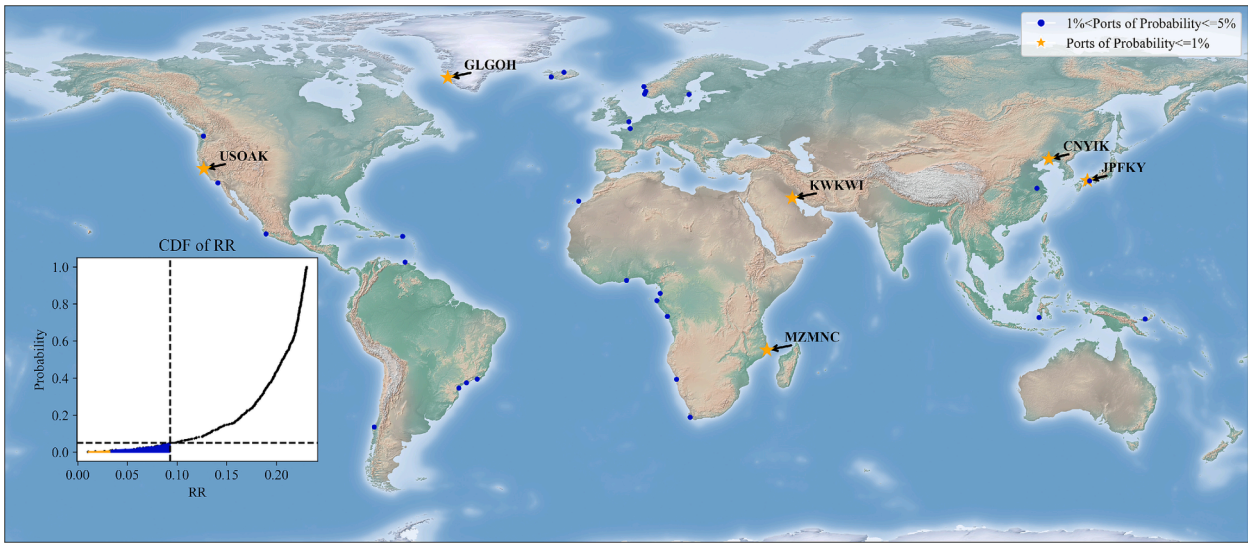

Fig. 8. The distribution of the ports based on the RR in the BFRR-based cascade.

Table 5
The resilience metrics for the 7 ports in the BFRR-based cascade that have the greatest impact on network robustness.

Initial failed port	The size of the GWCC	WE	RR
CNSHA	634	0.0753	0.1514
SGSIN	649	0.0779	0.1399
DEHAM	644	0.0750	0.1797
NLRTM	614	0.0675	0.1315
BEANR	647	0.0694	0.1626
KRPUS	643	0.0804	0.1592
MAPTM	669	0.0779	0.1765

example, as the largest port in this study in terms of weight, the Port of Singapore receives a RR of 0.1399 after redistribution, corresponding to a redundancy of 2,300,000 TEUs. Combined with the size of the GWCC and the WE in this scenario, although the failure of the Port of Singapore leads the network robustness and connectivity of the GCSN to drop, the BFRR-based cascading process allows the network to maintain a certain level of redundancy. This observation underscores a key characteristic of the BFRR approach: 1) on

the one hand, multi-objective redistribution decisions do affect more ports and even cause them to be overloaded, 2) on the other hand, the participation of more ports also increases the safety backup of the system. Therefore, the resilience of the GCSN needs to be critically assessed based on the above results: 1) from an economic point of view, the BFRR-based cascade indeed causes significant disruptions within the network and results enormous economic losses in the international shipping market; 2) however, from a safety and risk control perspective, this strategy is proved to be able to spread out the cascading failures and the remaining GCSN still have a certain degree of safety redundancy to cope with the more unknown risks.

Additionally, this study also turns attention to ports with the smaller RR values within the GCSN, as depicted in Fig. 8 and Table 6. Notably, when using ports like Nacala and Nuuk as the initial failed ports, which are located in Mozambique and Greenland, the GCSN experiences low RR values. This phenomenon suggests a relatively weaker ability to cope with unforeseen risks from these ports, possibly leading to cargo wastage. However, this does not necessarily indicate a lack of redundancy in the GCSN but rather underscores the geographical limitations and the restricted number of accessible ports for Nacala and Nuuk. Furthermore, the ports listed in Table 6 exhibit high levels of network robustness. This observation suggests that failures at these ports, while challenging locally, do not significantly disrupt the resilience of the GCSN as a whole. Therefore, from a global socio-economic standpoint, a very low redundancy at specific ports is not necessarily translated into major concerns. Nevertheless, local stakeholders should be mindful of the low redundancy levels at these ports, as the unmanaged risks can strain local systems and adversely affect communities in those regions.

4.1.3. DFRR-based cascade

Different from the BFRR, the DFRR-based cascade uniquely selects a single port as the target for load redistribution from failed or overloaded ports. In this scenario, all global ports also have a capacity multiplier set at 1.3. The size of the GWCC and the WE of the original GCSN are 686 and 0.092, respectively. Applying the DFRR to simulate the cascading failures, 686 ports are iterated sequentially as initial failed ports, and the size of the GWCC, the WE and the RR are calculated after each port iteration. Based on the CDF of the size of the GWCC, the WE and the RR, the ports with the smallest values are highlighted in Figs. 9 - 11. Compared with the results presented in Section 4.1.2, the ports depicted in Figs. 9 and 10 are also mainly located in Europe and Asia. Detailed resilience metrics for these ports are shown in Table 7.

From Table 7, a distinctive feature of the DFRR-based cascade is the smaller number of overloaded ports, resulting in less reduction in both the size of the GWCC and the WE when compared to the BFRR-based cascade. Particularly, an interesting finding is that for the cascade failures triggered by the Port of Singapore as the initial failed port, the DFRR-based cascade reduces the WE of the network to 0.0439, less than the result obtained in the BFRR-based cascade. However, the size of the GWCC is 677 for the DFRR, compared to 649 for the BFRR. This disparity underscores the role of important ports in the cascading process. Important ports, often integral to the shortest paths in the network due to their transshipment and connectivity functions, are preferentially overloaded in the DFRR-based cascade. In contrast, the BFRR approach, despite leading to a higher number of overloaded ports, still predominantly affects those crucial ports which are integral to maintaining network efficiency and connectivity. Therefore, these findings demonstrate how both redistribution rules, despite their differences in port selection and load redistribution, effectively reflect commercial preferences in practice.

Similarly, turning attention to the performance of RR in the DFRR-based cascade, a notable characteristic is exhibited in the GCSN: it effectively avoids scenarios where goods cannot be redistributed, as indicated by the RR values consistently remaining above zero. This outcome is attributed to the interconnected nature of the modern shipping network. Under the DFRR approach, reserve capacity of each port is utilized sequentially until a port capable of accommodating the remaining load is found. The interconnectedness of GCSN ensures that there is a high probability at least one port is available, effectively avoiding a total halt in the network operations. However, the approach challenges the redundancy of the network. As indicated in Tables 7 and 8, the RR values in a DFRR-based cascade tend to be lower than those in the BFRR-based cascade. This observation leads to two key insights regarding the economic and risk control aspects of the DFRR-based cascade: 1) Economically, the DFRR strategy results in fewer overloaded ports. This outcome is beneficial as it maintains the overall functionality and connectivity of most ports in the network, thus supporting the smooth operation of global shipping activities; 2) In terms of risk control, the DFRR prevents a complete network collapse, but with less safety redundancy due to the single-target strategy. Consequently, the network may become more vulnerable to other unknown risks and disruptions. The limited redundancy makes the network more susceptible to cascading failures.

4.1.4. Scenario analysis and comparison

To enhance the credibility of this study, 5 significant historical port disruption events with significant impacts are selected for scenario analysis. In each scenario, the capacity multiplier for all global ports is set at 1.3, consistent with Section 4.1.2 and Section

Table 6
The resilience metrics of 6 ports with the smallest RR in the BFRR-based cascade.

Initial failed port	The size of the GWCC	WE	RR
MZMNC	685	0.0918	0.0103
GLGOH	684	0.0916	0.0106
CNYIK	685	0.0919	0.0178
USOAK	678	0.0904	0.0269
KWKWI	685	0.0919	0.0323
JPFKY	685	0.0918	0.0331

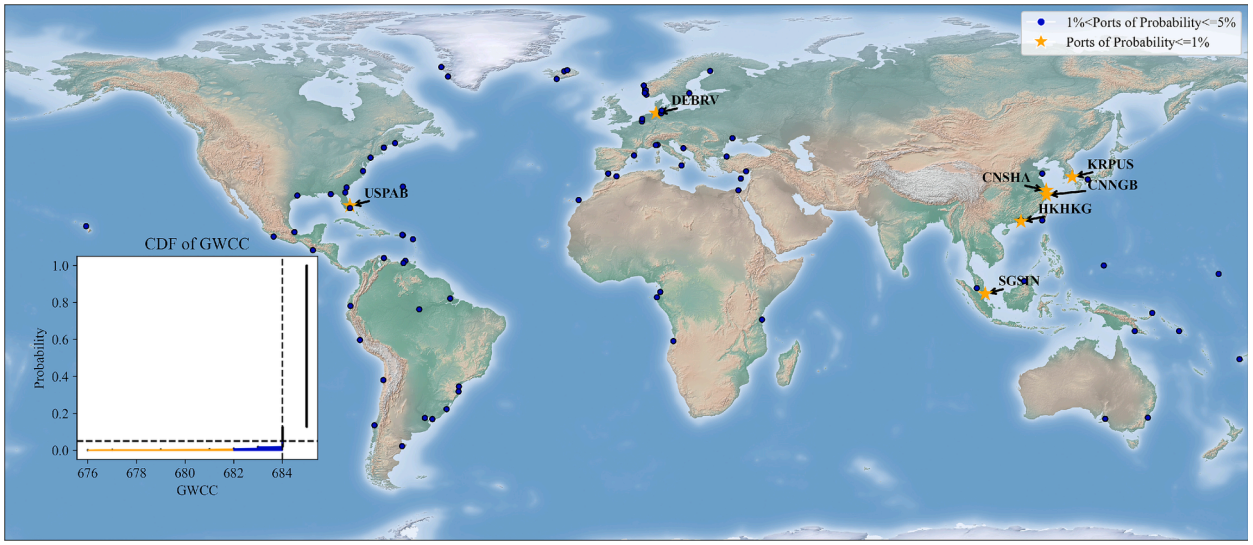

Fig. 9. The distribution of the ports based on the size of the GWCC in the DFRR-based cascade.

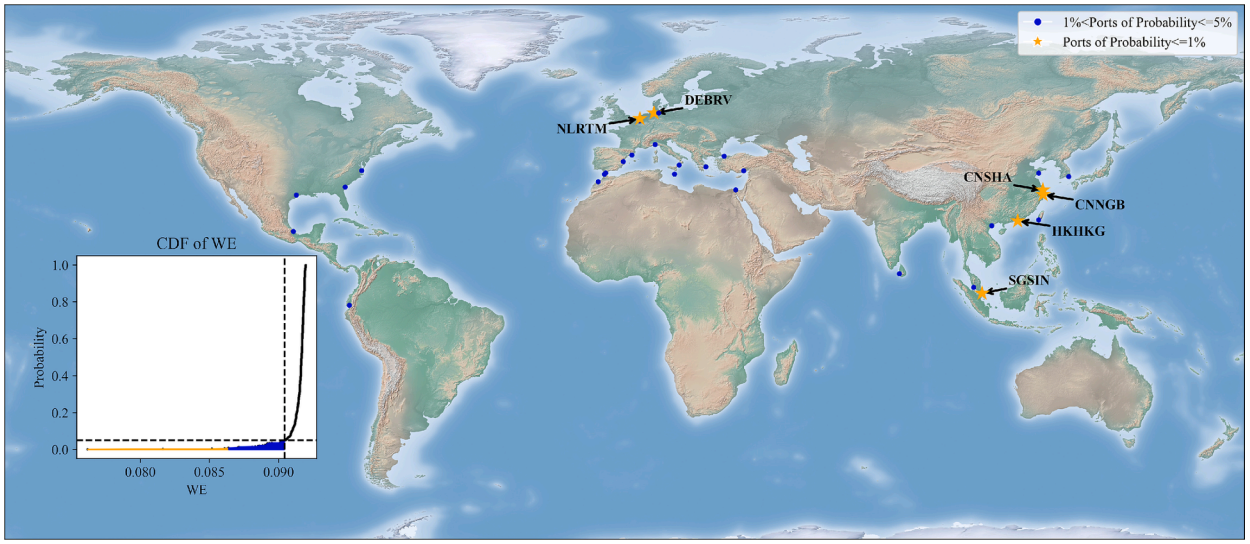

Fig. 10. The distribution of the ports based on the WE in the DFRR-based cascade.

4.1.3. The BFRR and DFRR methods are then applied to simulate cascading failures triggered by these events. The propagation of cascading failures is visualized in Figs. 12 and 13, where line color and thickness indicate the order and volume of load redistribution—darker lines represent earlier redistribution, and thicker lines denote larger load transfers. Additionally, the MSA method (introduced by Xu et al. (2024)) is simulated across the same 5 events to further illustrate the comparative analysis. Resilience metrics for each scenario are presented in Table 9.

Consistent with observations in Sections 4.1.2 and 4.1.3, the BFRR-based redistribution typically leads to a greater reduction in network resilience due to its multi-target redistribution strategy, which is a commonly used approach in real-world scenarios to spread risks more quickly. In contrast, the DFRR-based load redistribution increases the burden on a single port, thus challenging the redundancy. For instance, the explosion in Beirut—a major port accident caused by the explosion of ammonium nitrate—disrupted port operations and required cargo to be redirected to other ports or temporary storage sites. This accident notably impacted supply chains in the Mediterranean region, as visualized in Fig. 12 (a) and 13 (a). Simulation results closely align with these real events: Beirut's closure led to increased loads on nearby ports, such as Lebanon's Tripoli port, Cyprus, and Turkey (Wills, 2020). However, the limited capacity of these ports constrained the overall damage to the GCSN. A similar phenomenon occurred during the 2024 Baltimore port bridge collapse, caused by a collision of the containership Dali with the Francis Scott Key Bridge, which led to the port's temporary closure. As one of the major U.S. ports handling cars and coal, this accident forced nearby ports to absorb additional loads, though it

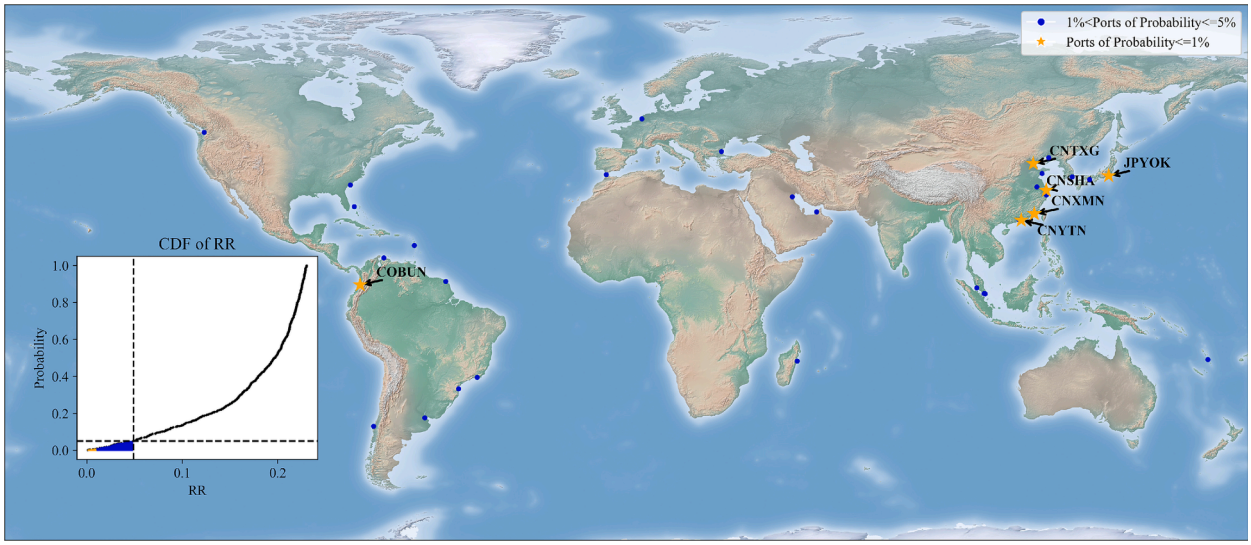

Fig. 11. The distribution of the ports based on the RR in the DFRR-based cascade.

Table 7
The resilience metrics for the 7 ports in the DFRR-based cascade that have the greatest impact on network robustness.

Initial failed port	The size of the GWCC	WE	RR
SGSIN	677	0.0762	0.0108
CNSHA	679	0.0816	0.0065
CNNGB	681	0.0852	0.0279
DEBRV	676	0.0861	0.1509
HKHKG	682	0.0863	0.0734
NLRTM	684	0.0864	0.0361
KRPUS	682	0.0864	0.0259

Table 8
The resilience metrics for the 6 ports with the smallest RR in the DFRR-based cascade.

Initial failed port	The size of the GWCC	WE	RR
CNXMN	685	0.0911	0.0011
JPYOK	685	0.0908	0.0019
CNYTN	684	0.0892	0.0032
CNSHA	679	0.0816	0.0065
CNTXG	685	0.0915	0.0088
COBUN	685	0.0916	0.0103

had limited effects on global container trade (Bedigan et al., 2024), as shown in Fig. 12 (e). Nevertheless, minor reductions in the GWCC size and the WE are observed, consistent with reports that this event's impact on the maritime industry is more related to safety than to economic cascading effects.

Furthermore, during the COVID-19 pandemic, several major ports, including Shanghai, Ningbo, and Yantian, were forced to shut down due to local health policies, creating backlogs of cargo. Major shipping companies such as Maersk and Mediterranean Shipping Company have had to skip these closed ports, increasing the load on others. As shown in Figs. 12 and 13, these redistributions caused significant overloads in the East-South Asia region. Shanghai port, one of the world's largest, redistributed its load four times. Although this study explores cascading failures under extreme cases where all port loads are redistributed, it significantly highlights the critical role of Shanghai port in network resilience. These insights have prompted the shipping industry to consider strategies such as near-shore outsourcing and expanding port capacities to manage future crises (Lindstrand, 2022).

Compared to traditional non-iterative algorithms (e.g., Xu et al. (2022), Bai et al. (2023) and this study), the MSA method balances load redistribution more effectively by iteratively adjusting load transfers based on a cost function until convergence is reached. Specifically, the MSA method redistributes load through a mixed number of routes (e.g., 3 routes, as referenced in (Xu et al., 2024)), prioritizing nearer ports based on a distance-first principle.

Table 9 summarizes five cases that illustrate the distinct characteristics of each redistribution rule and their contextual fitness. From a robustness perspective, the MSA method demonstrates a smaller reduction in WE during disruptions at medium-sized ports (e.g.,

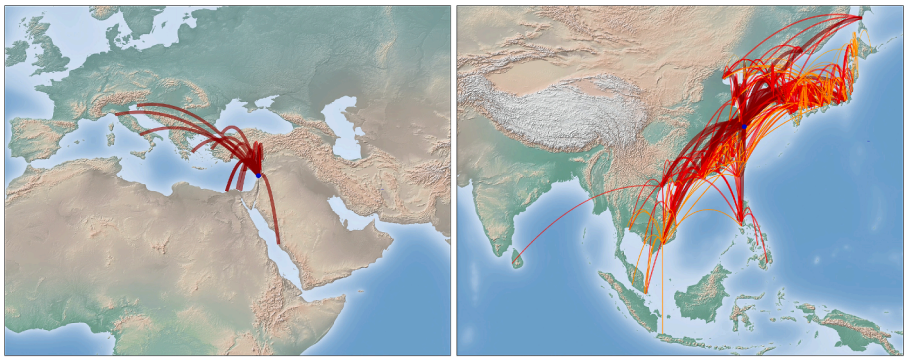

(a) the 2020 Beirut port explosion (b) the Shanghai port lockdown during COVID-19

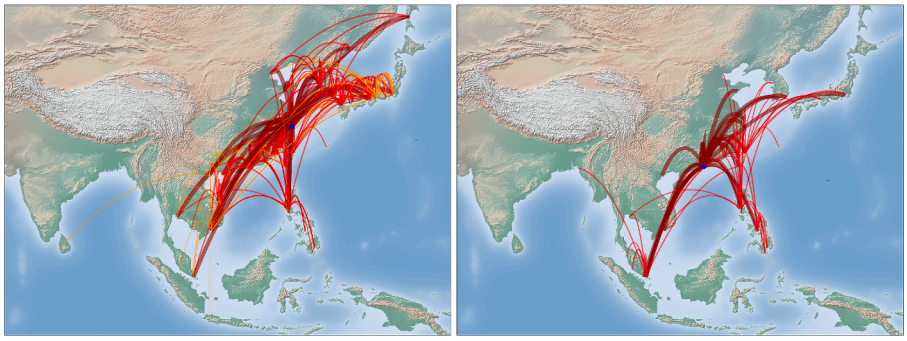

(c) the Ningbo port lockdown during COVID-19 (d) the Yantian port lockdown during COVID-19

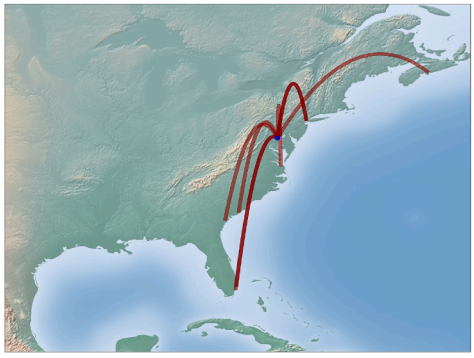

(e) the 2024 collision at Baltimore port bridge

Fig. 12. Cascading failure propagation triggered by 5 historical port disruption events globally with the BFRR.

Beirut Port and Baltimore Port) than both the BFRR and DFRR methods. However, in scenarios involving large-sized port disruptions (e.g., Shanghai Port, Ningbo Port, and Yantian Port), the MSA approach results in fewer port overloads than the BFRR but more than the DFRR. Practically, the BFRR employs an approximate omni-target selection principle, redistributing loads proportionally to all qualified ports, which can lead to nearby small ports becoming overloaded due to limited reserve capacity. In contrast, the DFRR and MSA methods, which constrain the number of redistribution targets, reduce the likelihood of port overloads. Despite this, the BFRR still offers a significant advantage in maintaining a higher level of RR, ensuring sufficient backup capacity to handle future disruptions. However, iterative methods like the MSA may face challenges related to computational complexity, particularly as the number of redistribution targets increases, leading to higher computation and simulation times.

4.2. Case study

Based on the results in Section 4.1.1, the ports of Singapore, Busan, Shanghai, Rotterdam and Antwerp have been identified as the top 5 ports in the importance assessment. The failures of these five ports also show greater damage to the resilience of the network in the BFRR and the DFRR based cascading scenarios. To further expand the scope of interest ranging from Asia and Europe to America, a case study involving the Port of New York, which is the top-ranked port in the Americas in terms of importance, is conducted in this

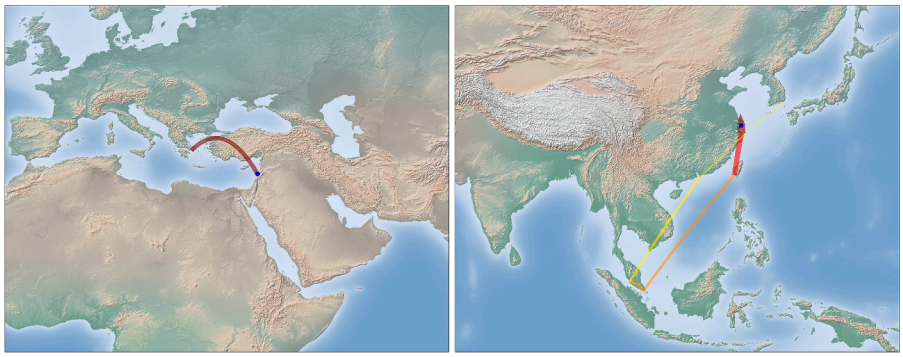

(a) the 2020 Beirut port explosion (b) the Shanghai port lockdown during COVID-19

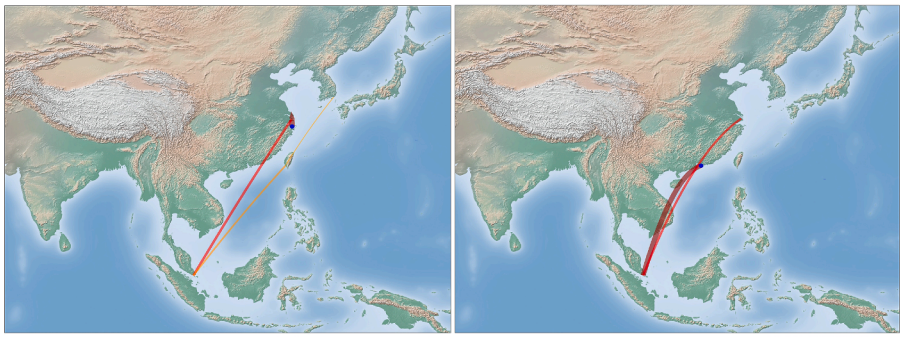

(c) the Ningbo port lockdown during COVID-19 (d) the Yantian port lockdown during COVID-19

(e) the 2024 collision at Baltimore port bridge

Fig. 13. Cascading failure propagation triggered by 5 historical port disruption events globally with the DFRR.

section.

In Section 4.2, the cascading failures are in-depth analysed by changing the value of the capacity multiplier in the GCSN from a range of 1.01 to 2.0. To clearly illustrate the correlation between network resilience and the capacity multiplier, following several experiments, an increment of 0.01 is set for the capacity multiplier within the range of 1.01 to 1.2, and an increment of 0.05 within the range of 1.2 to 2.0. Each port thus contains results for 36 distinct values of the capacity multiplier.

4.2.1. Performance of key ports (BFRR)

Fig. 14 exhibits the changes in resilience metrics with capacity multipliers for the failures of these six ports under the BFRR-based cascade. Overall, the resilience in all scenarios experiences a fluctuating increase, then the size of the GWCC and the WE stabilise at a certain level, and the RR continues to rise. The resilience of the network is analysed in terms of both robustness and redundancy. Particularly, the resilience of the GCSN exhibits two characteristics in the BFRR-based cascade: 1) sensitivity and 2) threshold effects.

For the ports of Singapore, Busan, Rotterdam, and Antwerp, the GWCC and the WE drastically fluctuate when the capacity multiplier grows from 1.01 to 1.2. Specifically, with a relatively smaller λ, the GCSN has insufficient safety backup. Loads from the initial failed port cannot be fully absorbed by the whole network and even lead to significant overloads among global ports. Such phenomena can be illustrated by the values of GWCC and WE approximately being 0 and the negative value of RR. As λ continues to

Table 9
The resilience metrics of 5 scenarios.

Event	Rule	GWCC size	ΔGWCC size	Reduction rate of GWCC size	WE	ΔWE	Reduction rate of WE	RR
2020 Beirut Port Explosion	BFRR	684	2	0.29 %	0.0909	0.0011	1.15 %	0.2019
	DFRR	685	1	0.15 %	0.0911	0.0009	0.99 %	0.0825
	MSA	683	3	0.44 %	0.0911	0.0009	0.93 %	0.1084
Shanghai Port Lockdown during COVID-19	BFRR	634	52	7.58 %	0.0753	0.0166	18.08 %	0.1514
	DFRR	679	7	1.02 %	0.0816	0.0104	11.26 %	0.0065
	MSA	679	27	3.94 %	0.0786	0.0133	11.26 %	0.0907
Ningbo Port Lockdown during COVID-19	BFRR	666	20	2.92 %	0.0803	0.0117	12.71 %	0.1642
	DFRR	681	5	0.73 %	0.0852	0.0068	7.39 %	0.0279
	MSA	669	17	2.48 %	0.824	0.0096	10.43 %	0.1009
Yantian Port Lockdown during COVID-19	BFRR	680	6	0.87 %	0.0886	0.0034	3.72 %	0.1862
	DFRR	684	2	0.29 %	0.0892	0.0028	3.03 %	0.0032
	MSA	683	3	0.44 %	0.0880	0.0040	4.36 %	0.0539
2024 Baltimore Port Bridge Collision	BFRR	685	1	0.15 %	0.0917	0.0003	0.31 %	0.1856
	DFRR	685	1	0.15 %	0.0917	0.0003	0.31 %	0.1143
	MSA	686	0	0	0.0920	0	0	0.1249

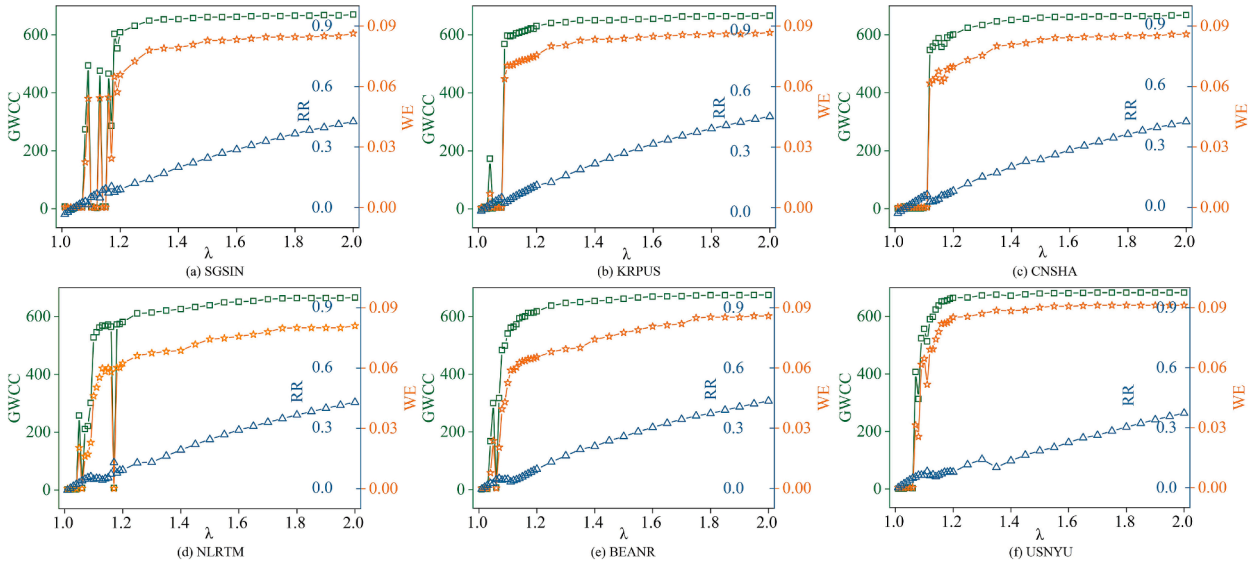

Fig. 14. The resilience metrics in the BFRR-based cascade triggered by different ports. (a) Singapore Port; (b) Busan Port; (c) Shanghai Port; (d) Rotterdam Port; (e) Antwerp Port; (f) New York Port.

increase, significant fluctuations occur in Fig. 14. For example, in the case of the cascading failures triggered by Singapore Port, when the capacity multiplier increases from 1.07 to 1.1, the size of the GWCC in the network increases from 6 to 494 and then decreases to 7. This sensitivity to changes in the capacity multiplier is indicative of the complexity of the topology structure of the shipping network. Due to the interconnectedness and heterogeneity of ports in the shipping network, the load redistribution has an unintuitive non-linear character. Theoretically, the resilience of the network is expected to improve with the increasing capacity multiplier, which could be manifested by a continued increase in the size of the GWCC. In this study, the capacity increase is not uniform across all ports; those with higher initial capacity tend to gain more reserve capacity. The immediate impact is that larger ports prevent the transfer of load to nearby smaller ports, significantly easing the pressure on those smaller ports. As a result, these smaller ports no longer need to be redistributed or overloaded. This explains the rise in both the GWCC and WE at this point. However, this unbalanced capacity growth will continue to attract more loads and increase pressure on the larger ports. Once these attracted loads exceed capacity limits and overload the larger ports, the surrounding smaller ports will therefore need to absorb the additional loads. Furthermore, due to the significant differences in reserve capacity between two different groups of ports, these small ports are vulnerable and overloading of these small ports will cause a rapid decline in GWCC and WE values.

In network flow theory, if traffic is unevenly distributed in a network, traffic may be attracted to specific nodes, leading to congestion. Such a phenomenon is also in line with the concept of Braess's Paradox, which states that the addition of extra capacity (e.g., on ports, links, etc.) in a network (e.g., transport network, shipping network, etc.) may instead lead to deterioration rather than improvement of the overall performance (Roughgarden and Tardos, 2002). The reason for this is that changes in the network form new game structures that dynamically change the redistribution process. Therefore, in the GCSN, this paradox manifests as ports with

increased capacity attract more load, thereby causing temporary overloads. As a result, the cascading failures in such complex traffic networks have black-box-like propagation properties. Specific propagation processes within the network, although theoretically observable, would be practically challenging to track the movements in a large and dense traffic interconnection network. Therefore, another characteristic of "threshold effects" can provide additional insights into the propagation behaviour of cascading failures within the GCSN. In light of this challenge, the models in this work provide insightful solutions by proposing a two-objective optimisation as follows.

Firstly, when analysing the resilience of the GCSN in terms of network connectivity and robustness, the first threshold can be observed at lower values of the capacity multiplier, i.e., a small increase in capacity may lead to a large rise in initial resilience. To elucidate this effect, notable examples involving the ports of Shanghai, Busan, Antwerp and New York are delved. When the port of Shanghai is treated as the initial failed port, an increase of capacity multipliers from 1.11 to 1.12 correspond to a significant improvement in the size of the GWCC from 7 to 548. A similar trend is observed for Busan, where the GWCC size increases from 5 to 568 with a capacity multiplier change from 1.08 to 1.09. The WE value in each scenario is consistent with the change in the size of the GWCC. Therefore, the appearance of the first threshold effect is symptomatic of the network being resilient. Additionally, it underscores the dynamic interplay between capacity and network performance.

Furthermore, as the stakeholders of ports, another key concern is to know how to manage ports in a way that keeps resilient and avoids the high costs in construction and the waste of resources in maintenance. Therefore, the second threshold effect would aim to address this issue, which is reflected in the stabilisation point of the network resilience. For instance, for the Port of Singapore, the second threshold is identified at a capacity multiplier of $\lambda = 1.35$. At this point, the size of the GWCC and the WE stabilise at more than 95 % of original level, and the network exhibits positive redundancy, indicating stable resilience. Similarly, a value of around 1.3 would be applicable to the remaining five ports as well. Therefore, from a practical standpoint, these two threshold values offer vital guidelines for port construction and risk prevention. The first threshold ensures basic network resilience by maintaining sufficient capacity, where the second threshold promotes a more stable and efficient network performance without unnecessary resource expenditure. Ports should aim to meet the first threshold and strive to meet the second for optimal performance. This approach allows for tailored port development strategies, taking into account individual trade volumes and network roles, thereby enhancing overall network resilience and efficiency.

4.2.2. *Performance of key ports (DFRR)*

In the application of the DFRR to the GCSN, focusing on the ports of Singapore, Busan, Shanghai, Rotterdam, Antwerp, and New York, distinct patterns of resilience are observed as depicted in Fig. 15. Compared to the BFRR-based cascade, the DFRR-based cascade process is more straightforward, with ports overloading one after the other, and therefore this will enable an in-depth analysis of the propagation process of the DFRR-based cascading failures.

Firstly, there is a clear stepwise threshold effect in the DFRR-based cascade process. For example, it is obvious that the robustness of the network for these six scenarios remains constant in the beginning and the network redundancy continues to increase. Using Fig. 15 (a) as an example to explain this effect, below a capacity multiplier of 1.07, the DFRR-based cascade triggered by Singapore follows a consistent path, maintaining the GWCC size and the WE at 571 and 0.0174, respectively, while network redundancy remains negative. This pattern occurs because the DFRR consistently selects the highest importance-ranked port among eligible ports, leading to a fixed redistribution path until no further eligible ports are available. Negative redundancy indicates that the load from the initial failed port

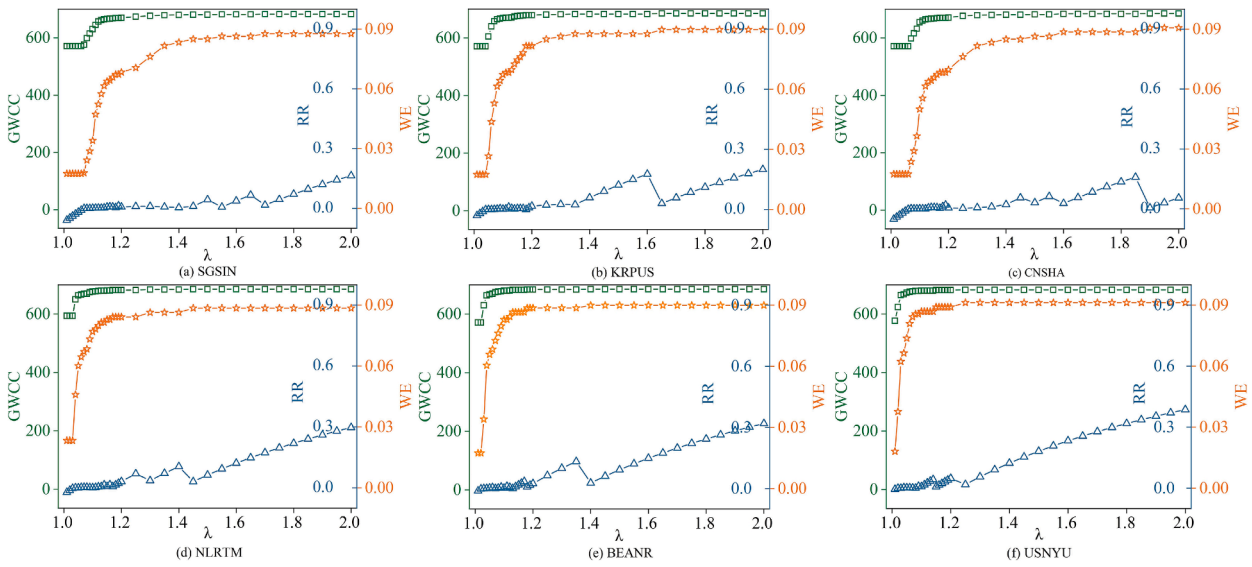

Fig. 15. The resilience metrics in the DFRR-based cascade triggered by different ports. (a) Singapore Port; (b) Busan Port; (c) Shanghai Port; (d) Rotterdam Port; (e) Antwerp Port; (f) New York Port.

cannot be fully absorbed along this path. When the capacity reaches a certain threshold, a port on this path, named as port A, ceases to be overloaded. It signifies that the preceding ports can now handle loads from the initial failed port, eliminating the need for further redistribution. Therefore, the network starts to be resilient, as evidenced by the fact that the size the GWCC and the WE begin to rise, and the RR turns to be positive.

Subsequently, as the capacity multiplier reaches the second critical value of about 1.2 (i.e., the second threshold), the robustness of the network stabilises at a certain level. Post this threshold, a unique feature of the DFRR-based cascade emerges: a sudden drop in redundancy with increased capacity. Continuing with the example of Fig. 15(a), one reason of this drop is that the number of participating ports diminishes. At a capacity multiplier of 1.65, the cascading failures triggered by the Port of Singapore redistribute the load to the ports of Busan, Shanghai and Kaohsiung, and cause overloads at the ports of Busan and Shanghai. However, when the capacity multiplier increases to 1.7, the ports involved are Busan and Shanghai and only Busan is overloaded, with the cascade stopping at Shanghai. Therefore, when the capacity multiplier is equal to 1.65, the redundancy of the network is 355,777 TEUs, and the total capacity of the three participating ports is 5,315,123 TEUs. According to Equation (5), the RR at this time is 0.0669. However, when the capacity multiplier rises to 1.7, the redundancy of the network is 74,701 TEUs, and the total capacity of these two participating ports is 4,402,419 TEUs, with the RR of 0.0170. It can be found that as the number of participating ports decreases, the redundancy of the network decreases dramatically, so the network robustness is almost unchanged, while the RR drops abruptly.

Therefore, based on the above results, the DFRR likewise provides a theoretical basis for mitigating the cascading failures triggered by port disruptions. Compared with the BFRR, for the large ports such as Singapore, Busan and Shanghai, although theoretically the DFRR appears to result in fewer ports failing, the process requires filling up the ports on the redistribution path sequentially. This can lead to insufficient safety backups if the capacity of the ports is small. This observation suggests that ports within the GCSN should consider increasing their capacity multipliers beyond the commonly used 1.2 (Hossain et al., 2019) to enhance their ability to handle cascading disruptions effectively.

5. Discussions and implications

Based on the results in Section 4, the approach to model cascading failures based on the port importance assessment is deemed rational and reliable. In a large and complex shipping network system, the key to achieving the simulation of cascading is to identify the target ports and determine the load redistribution rules. Although acknowledging that a full simulation of real-world scenarios is challenging depending on the interaction of multiple political, human and economic factors, this study contributes a theoretical framework for advanced port assessment. It integrates multiple factors to approximate business behaviours in an ideal situation, pioneering two cascading failure simulation rules – the BFRR and the DFRR – each employing different methods for load redistribution and contributing to resilience development for the GCSN. Specifically, the BFRR simulates general multi-target load redistribution, increasing the redundancy and flexibility of the network, which helps to distribute overloading risks. In particular, in the event of a failure in a large port, the BFRR facilitates faster load redistribution to multiple ports, ensuring the continuity of goods flow. Therefore, by evaluating the impact of such a multi-target load redistribution strategy on the entire network, decision makers can implement policies that maximize overall benefits of the network and reduce the burden on individual ports, thereby increasing the resilience of the global network in the face of unpredictable challenges. The DFRR, on the other hand, focuses on using a single port's resources for centralized processing or further redistribution of goods. This approach is particularly well-suited for smaller ports or certain specialized cargo, where centralized transport to larger ports would be more efficient, secure and economical. Compared to the BFRR, this single-target model in the DFRR simplifies the decision-making process, making it easier to respond and adapt strategies emergency. This allows for quicker mitigation or prevention of cascading failures. Additionally, the DFRR can further help identify critical ports in the GCSN that can handle increased loads and stresses, thereby reducing the vulnerability of smaller ports and strengthening the resilience of the overall network.

Furthermore, the practical implications of this study are substantial. It highlights the significant impact of key port failures on the global shipping market, as evidenced by events like the 2020 Beirut port explosion, the COVID-19 related lockdowns of Shanghai, Ningbo, and Yantian ports, and the 2024 collision at Baltimore port bridge. These incidents resonate with the findings of this study, demonstrating the influence of port disruptions in regions on the resilience of the GCSN, which can be found from Fig. 12 to Fig. 13. The real-world repercussions of these events, e.g., shocks to the global supply chain and trade, validate results in this study, underscoring the importance of effective risk control and port management. Therefore, in this section, the insights for different stakeholders will be further clarified.

From a port perspective, effective risk warnings and accurate risk assessments are crucial for accident prevention. Enhancing the handling capacity of key ports, as suggested in Section 4.2, can bolster the overall resilience of the GCSN. In practice, capacity improvement extends beyond physical expansion: it also encompasses optimizing industrial equipment, efficiently allocating resource, advancing digitalization and automation, and integrating multimodal operations. These technological advancements not only streamline port operations but also reinforce the stability and resilience of the global shipping network.

From the perspective of shipping companies, optimising route decisions and resource deployment are effective ways to reduce the impact of some link disruptions. The BFRR and the DFRR represent distinct decision-making preferences: the BFRR spreads risk and can enhance safety by reducing reliance on a single port, while the DFRR suits companies with centralized resource allocation, reducing scheduling and operational costs by unifying cargoes to major consolidation hubs.

From a national perspective, two topics should be brought to the forefront from this study: developing diversified and stable supply chain policies and investing in infrastructure. On a macro level, in the context of economic globalisation, diversified and stable supply chain policies rely on multi-regional cooperation. Although load redistribution targets may realistically give preference to ports in the

same country, redistribution of load within a country actually increases the pressure and risk on the national supply chain. For countries like Singapore, leveraging their transit role to ensure trade stability and continuity through enhanced resilience is crucial. In addition, to facilitate the enhancement of port capacity, governments should support the upgrading and construction of ports in terms of investment and policy, fostering sustainable development in the domestic port and shipping sectors, as indicated in the recommendations of Section 4.2.

6. Conclusions

The resilience of the GCSN is the basis for coping with unknown risks and ensuring the economic stability of the market. Distinguishing from the existing static studies, this study marks a significant advancement in the analysis of shipping network resilience by innovatively proposing two dynamic cascading failure models based on port importance assessment. To quantify the impact of the GCSN resilience by port disruptions, two robustness metrics, the size of the GWCC and the WE, and one redundancy metric are applied to 686 global ports to comprehensively reveal the extent to which each port failure disrupts the resilience of the GCSN. The results of this study can be summarised as follows: 1) based on port importance assessment, the BFRR and the DFRR are introduced as fundamental load redistribution models to simulate the port selection and load determination behaviours in a complex operational landscape, offering new perspectives on how load redistribution might occur in response to disruptions within the shipping network; 2) specifically, the BFRR contributes to risk diversification and enhances safety redundancy, while the DFRR prefers to contribute to centralised resource allocation and reduce cascading damage to the entire shipping network; 3) five historical events are then simulated to further compare the results in this study with real world values; 4) the BFRR exhibits sensitivity and a threshold effect in response to alterations in port capacity, with modifications in the game theory structure of the dynamic redistribution process confirming the presence of the Braess's Paradox in complex shipping networks; 5) comparatively, the DFRR demonstrates the more straightforward redistribution preference, with the result showing a stepwise threshold effect, which requires ports in the GCSN to upgrade their capacity to ensure safety redundancy.

The proposed framework in this study lays the groundwork for dynamically assessing shipping network resilience by quantifying the impact of port failures on the GCSN. It also offers practical insights for various stakeholders, underlining the importance of strategic load redistribution in maintaining network resilience. Moving forward, future research can be conducted by an expansion of this foundation to enhance resilience assessments both methodologically and practically. At the modelling level, incorporating both the BFRR and the DFRR into a hybrid model would more accurately capture real-world dynamics, despite the inherent uncertainties arising from the independence and heterogeneity of ports. More applications of traffic flow assignment theories offer a new perspective to simulate load redistribution in shipping networks, as demonstrated in a recent study by (Xu et al., 2024). Furthermore, current studies lack integration of real-time recovery dynamics in accessing shipping network resilience, highlighting a need for a comprehensive review of port recovery factors and the development of recovery functions to model these dynamics. From a practical application standpoint, resilience analyses of regional or national networks are attracting more attention and interest. However, fully accounting for the interactions within and between regions remains challenging. At the data level, more data sources (e.g., AIS data) are expected to be utilized in future research. Developing a hybrid service-AIS database would further enhance the research capabilities, enabling real-time monitoring and a more comprehensive assessment of global shipping networks. These advancements will deepen our understanding of resilience in shipping networks and improve the ability to mitigate disruptions effectively.

CRediT authorship contribution statement

Yuhao Cao: Writing – review & editing, Writing – original draft, Visualization, Software, Methodology, Formal analysis, Data curation, Conceptualization. **Xuri Xin:** Writing – review & editing, Validation, Supervision, Methodology, Conceptualization. **Pisit Jarumaneeroj:** Resources, Data curation. **Huanhuan Li:** Writing – review & editing, Methodology, Project administration. **Yinwei Feng:** Writing – review & editing, Validation, Software, Methodology. **Jin Wang:** Writing – review & editing, Validation, Supervision, Project administration. **Xinjian Wang:** Writing – review & editing, Validation, Supervision, Project administration. **Robyn Pyne:** Writing – review & editing, Supervision, Project administration. **Zaili Yang:** Writing – review & editing, Supervision, Project administration, Funding acquisition, Conceptualization.

Declaration of competing interest

The authors declare that they have no known competing financial interests or personal relationships that could have appeared to influence the work reported in this paper.

Acknowledgements

This research was funded by a European Research Council project under the European Union's Horizon 2020 research and innovation programme (TRUST CoG 2019 864724). The authors also gratefully acknowledge support from the National Natural Science Foundation of China [Grant no. 52101399], the Bolian Research Funds of Dalian Maritime University (Grant No. 3132023617) and the China Scholarship Council under Grant: 202308060322.

Data availability

Data will be made available on request.

References

Alipour, Z., Monfared, M.A.S., Zio, E., 2014. Comparing topological and reliability-based vulnerability analysis of Iran power transmission network. Proc. Inst. Mech. Eng. Part O: J. Risk Reliab. 228 (2), 139–151. https://doi.org/10.1177/1748006X13501652.

Bai, X., Ma, Z., Zhou, Y., 2023. Data-driven static and dynamic resilience assessment of the global liner shipping network. Transp. Res. Part E: Logist. Transp. Rev. 170, 103016. https://doi.org/10.1016/j.tre.2023.103016.

Baroud, H., Barker, K., Ramirez-Marquez, J.E., Rocco, C.M., 2015. Inherent costs and interdependent impacts of infrastructure network resilience. Risk Anal. 35 (4), 642–662. https://doi.org/10.1111/risa.12223.

Baroud, H., Barker, K., Ramirez-Marquez, J.E., Rocco S, C.M., 2014a. Importance measures for inland waterway network resilience. *Transportation Research Part E: Logistics and Transportation Review* 62, 55-67. Doi: 10.1016/j.tre.2013.11.010.

Baroud, H., Ramirez-Marquez, J.E., Barker, K., Rocco, C.M., 2014b. Stochastic measures of network resilience: Applications to waterway commodity flows. Risk Anal. 34 (7), 1317–1335. https://doi.org/10.1111/risa.12175.

Bedigan, M., Watling, T., Ross, A., 2024. Baltimore bridge collapse sparks trade disruption with unusable port – what economic impact will it have? Independent. https://www.independent.co.uk/news/world/americas/baltimore-bridge-global-trade-b2518942.html.

Calatayud, A., Mangan, J., Palacin, R., 2017. Vulnerability of international freight flows to shipping network disruptions: A multiplex network perspective. Transp. Res. Part E: Logist. Transp. Rev. 108, 195–208. https://doi.org/10.1016/j.tre.2017.10.015.

Crucitti, P., Latora, V., Marchiori, M., 2004. Model for cascading failures in complex networks. Phys. Rev. E 69 (4), 045104. https://doi.org/10.1103/PhysRevE.69.045104.

Cumelles, J., Lordan, O., Sallan, J.M., 2021. Cascading failures in airport networks. J. Air Transp. Manag. 92, 102026. https://doi.org/10.1016/j.jairtraman.2021.102026.

Dorogovtsev, S.N., Mendes, J.F.F., Samukhin, A.N., 2001. Giant strongly connected component of directed networks. Phys. Rev. E 64 (2), 025101. https://doi.org/10.1103/PhysRevE.64.025101.

Dou, B.-L., Wang, X.-G., Zhang, S.-Y., 2010. Robustness of networks against cascading failures. Physica A 389 (11), 2310–2317. https://doi.org/10.1016/j.physa.2010.02.002.

Duan, J., Li, D., Huang, H.-J., 2023. Reliability of the traffic network against cascading failures with individuals acting independently or collectively. Transp. Res. Part C Emerg. Technol. 147, 104017. https://doi.org/10.1016/j.trc.2023.104017.

Dui, H., Zheng, X., Wu, S., 2021. Resilience analysis of maritime transportation systems based on importance measures. Reliab. Eng. Syst. Saf. 209, 107461. https://doi.org/10.1016/j.ress.2021.107461.

Fan, D., Sun, B., Dui, H., Zhong, J., Wang, Z., Ren, Y., Wang, Z., 2022a. A modified connectivity link addition strategy to improve the resilience of multiplex networks against attacks. Reliab. Eng. Syst. Saf. 221, 108294. https://doi.org/10.1016/j.ress.2021.108294.

Fan, S., Yang, Z., Wang, J., Marsland, J., 2022b. Shipping accident analysis in restricted waters: Lesson from the Suez Canal blockage in 2021. Ocean Eng. 266. https://doi.org/10.1016/j.oceaneng.2022.113119.

Feng, Y., Wang, H., Xia, G., Cao, W., Li, T., Wang, X., Liu, Z., 2024a. A machine learning-based data-driven method for risk analysis of marine accidents. *Journal of Marine Engineering & Technology*, 1-12. Doi: 10.1080/20464177.2024.2368914.

Feng, Y., Wang, X., Chen, Q., Yang, Z., Wang, J., Li, H., Xia, G., Liu, Z., 2024b. Prediction of the severity of marine accidents using improved machine learning. Transp. Res. Part E: Logist. Transp. Rev. 188, 103647. https://doi.org/10.1016/j.tre.2024.103647.

Fu, X., Pace, P., Aloi, G., Yang, L., Fortino, G., 2020. Topology optimization against cascading failures on wireless sensor networks using a memetic algorithm. Comput. Netw. 177, 107327. https://doi.org/10.1016/j.comnet.2020.107327.

Gadhia, H.K., Kotzab, H., Prockl, G., 2011. Levels of internationalization in the container shipping industry: An assessment of the port networks of the large container shipping companies. J. Transp. Geogr. 19 (6), 1431–1442. https://doi.org/10.1016/j.jtrangeo.2011.07.016.

Gu, Y., Fu, X., Liu, Z., Xu, X., Chen, A., 2020. Performance of transportation network under perturbations: Reliability, vulnerability, and resilience. Transp. Res. Part E: Logist. Transp. Rev. 133, 101809. https://doi.org/10.1016/j.tre.2019.11.003.

Gu, B., Liu, J., 2023. A systematic review of resilience in the maritime transport. Int. J. Log. Res. Appl. 1–22. https://doi.org/10.1080/13675567.2023.2165051.

Guo, X., Du, Q., Li, Y., Zhou, Y., Wang, Y., Huang, Y., Martinez-Pastor, B., 2023. Cascading failure and recovery of metro–bus double-layer network considering recovery propagation. Transp. Res. Part D: Transp. Environ. 122, 103861. https://doi.org/10.1016/j.trd.2023.103861.

Hossain, N.U.I., Nur, F., Hosseini, S., Jaradat, R., Marufuzzaman, M., Puryear, S.M., 2019. A Bayesian network based approach for modeling and assessing resilience: A case study of a full service deep water port. Reliab. Eng. Syst. Saf. 189, 378–396. https://doi.org/10.1016/j.ress.2019.04.037.

Hosseini, S., Ivanov, D., Dolgui, A., 2019. Review of quantitative methods for supply chain resilience analysis. Transp. Res. Part E: Logist. Transp. Rev. 125, 285–307. https://doi.org/10.1016/j.tre.2019.03.001.

Jarumaneeroj, P., Ramudhin, A., Barnett Lawton, J., 2023. A connectivity-based approach to evaluating port importance in the global container shipping network. Marit. Econ. Logist. 25 (3), 602–622. https://doi.org/10.1057/s41278-022-00243-9.

Jiang, L., Wang, G., Feng, X., Yu, T., Lei, Z., 2024. Study on cascading failure vulnerability of the 21st-century Maritime Silk Road container shipping network. J. Transp. Geogr. 117, 103891. https://doi.org/10.1016/j.jtrangeo.2024.103891.

Kang, L., Wu, W., Yu, H., Su, F., 2022. Global container port network linkages and topology in 2021. Sensors 22 (15), 5889. https://doi.org/10.3390/s22155889.

Latora, V., Marchiori, M., 2001. Efficient behavior of small-world networks. Phys. Rev. Lett. 87 (19), 198701. https://doi.org/10.1103/PhysRevLett.87.198701.

Lee, C.-Y., Song, D.-P., 2017. Ocean container transport in global supply chains: Overview and research opportunities. Transp. Res. B Methodol. 95, 442–474. https://doi.org/10.1016/j.trb.2016.05.001.

Lindstrand, C., 2022. UPDATED: COVID-19 disruptions in major China Ports. Mohawk Global. https://mohawkglobal.com/global-news/covid-19-disruptions-in-major-china-ports/.

Liu, X., Pan, L., Stanley, H.E., Gao, J., 2017. Controllability of giant connected components in a directed network. Phys. Rev. E 95 (4), 042318. https://doi.org/10.1103/PhysRevE.95.042318.

Liu, H., Tian, Z., Huang, A., Yang, Z., 2018. Analysis of vulnerabilities in maritime supply chains. Reliab. Eng. Syst. Saf. 169, 475–484. https://doi.org/10.1016/j.ress.2017.09.018.

Liu, Q., Yang, Y., Ke, L., Ng, A.K.Y., 2022a. Structures of port connectivity, competition, and shipping networks in Europe. J. Transp. Geogr. 102, 103360. https://doi.org/10.1016/j.jtrangeo.2022.103360.

Liu, Q., Yang, Y., Ng, A.K.Y., Jiang, C., 2023. An analysis on the resilience of the European port network. Transp. Res. A Policy Pract. 175, 103778. https://doi.org/10.1016/j.tra.2023.103778.

Liu, S., Yin, C., Chen, D., Lv, H., Zhang, Q., 2022b. Cascading failure in multiple critical infrastructure interdependent networks of syncretic railway system. IEEE Trans. Intell. Transp. Syst. 23 (6), 5740–5753. https://doi.org/10.1109/TITS.2021.3057404.

Motter, A.E., Lai, Y.-C., 2002. Cascade-based attacks on complex networks. Phys. Rev. E 66 (6), 065102. https://doi.org/10.1103/PhysRevE.66.065102.

Murray-tuite, P.M., Year. A Comparison of Transportation Network Resilience under Simulated System Optimum and User Equilibrium Conditions. *Proceedings of the 2006 Winter Simulation Conference*, 1398-1405. Doi: 10.1109/WSC.2006.323240.

Newman, M.E.J., Strogatz, S.H., Watts, D.J., 2001. Random graphs with arbitrary degree distributions and their applications. Phys. Rev. E 64 (2), 026118. https://doi.org/10.1103/PhysRevE.64.026118.

Peng, P., Cheng, S., Chen, J., Liao, M., Wu, L., Liu, X., Lu, F., 2018. A fine-grained perspective on the robustness of global cargo ship transportation networks. J. Geogr. Sci. 28 (7), 881–889. https://doi.org/10.1007/s11442-018-1511-z.
Qian, Y., Wang, B., Xue, Y., Zeng, J., Wang, N., 2015. A simulation of the cascading failure of a complex network model by considering the characteristics of road traffic conditions. Nonlinear Dyn. 80 (1), 413–420. https://doi.org/10.1007/s11071-014-1878-z.
Qin, Y., Guo, J., Liang, M., Feng, T., 2023. Resilience characteristics of port nodes from the perspective of shipping network: Empirical evidence from China. Ocean Coast. Manag. 237, 106531. https://doi.org/10.1016/j.ocecoaman.2023.106531.
Roughgarden, T., Tardos, É., 2002. How bad is selfish routing? J. ACM 49 (2), 236–259. https://doi.org/10.1145/506147.506153.
Sambowo, A.L., Hidayatno, A., 2021. Resilience index development for the manufacturing industry based on robustness, resourcefulness, redundancy, and rapidity. IJTech 12 (6), 1177. https://doi.org/10.14716/ijtech.v12i6.5229.
Sørensen, J.D., Rizzuto, E., Narasimhan, H., Faber, M.H., 2012. Robustness: Theoretical framework. Struct. Eng. Int. 22 (1), 66–72. https://doi.org/10.2749/101686612X13216060213554.
Tang, L., Jing, K., He, J., Stanley, H.E., 2016a. Complex interdependent supply chain networks: Cascading failure and robustness. Physica A 443, 58–69. https://doi.org/10.1016/j.physa.2015.09.082.
Tang, X., Liu, J., Hao, X., 2016b. Mitigate cascading failures on networks using a memetic algorithm. Sci. Rep. 6 (1), 38713. https://doi.org/10.1038/srep38713.
Tsiotas, D., Polyzos, S., 2018. Effects in the network topology due to node aggregation: Empirical evidence from the domestic maritime transportation in Greece. Physica A 491, 71–88. https://doi.org/10.1016/j.physa.2017.08.130.
UNCTAD, 2023. Review of Maritime Transport 2023. United Nations Conference on Trade and Development, New York, United States of America.
Viljoen, N.M., Joubert, J.W., 2016. The vulnerability of the global container shipping network to targeted link disruption. Physica A 462, 396–409. https://doi.org/10.1016/j.physa.2016.06.111.
Wang, W.-X., Chen, G., 2008. Universal robustness characteristic of weighted networks against cascading failure. Phys. Rev. E 77 (2), 026101. https://doi.org/10.1103/PhysRevE.77.026101.
Wang, N., Wu, N., Dong, L.-L., Yan, H.-K., Wu, D., 2016. A study of the temporal robustness of the growing global container-shipping network. Sci. Rep. 6 (1), 34217. https://doi.org/10.1038/srep34217.
Wills, K.L., 2020. Port of Beirut explosion forces diversion of vessels. Freight Waves. https://www.freightwaves.com/news/port-of-beirut-explosion-forces-diversion-of-vessels.
Wu, Z.X., Peng, G., Wang, W.X., Chan, S., Wong, E.W.M., 2008. Cascading failure spreading on weighted heterogeneous networks. J. Stat. Mech.: Theory Exp. 2008 (5). https://doi.org/10.1088/1742-5468/2008/05/P05013.
Wu, D., Wang, N., Yu, A., Wu, N., 2019. Vulnerability analysis of global container shipping liner network based on main channel disruption. Marit. Policy Manag. 46 (4), 394–409. https://doi.org/10.1080/03088839.2019.1571643.
Xu, M., Pan, Q., Muscoloni, A., Xia, H., Cannistraci, C.V., 2020. Modular gateway-ness connectivity and structural core organization in maritime network science. Nat. Commun. 11 (1), 2849. https://doi.org/10.1038/s41467-020-16619-5.
Xu, M., Deng, W., Zhu, Y., Lü, L., 2023. Assessing and improving the structural robustness of global liner shipping system: A motif-based network science approach. Reliab. Eng. Syst. Saf. 240, 109576. https://doi.org/10.1016/j.ress.2023.109576.
Xu, Y., Peng, P., Claramunt, C., Lu, F., Yan, R., 2024. Cascading failure modelling in global container shipping network using mass vessel trajectory data. Reliab. Eng. Syst. Saf. 249. https://doi.org/10.1016/j.ress.2024.110231.
Xu, X., Zhu, Y., Xu, M., Deng, W., Zuo, Y., 2022. Vulnerability analysis of the global liner shipping network: from static structure to cascading failure dynamics. Ocean Coast. Manag. 229, 106325. https://doi.org/10.1016/j.ocecoaman.2022.106325.
Zhou, Y., Wang, J., Huang, G.Q., 2019a. Efficiency and robustness of weighted air transport networks. Transp. Res. Part E: Logist. Transp. Rev. 122, 14–26. https://doi.org/10.1016/j.tre.2018.11.008.
Zhou, Y., Wang, J., Yang, H., 2019b. Resilience of transportation systems: Concepts and comprehensive review. IEEE Trans. Intell. Transp. Syst. 20 (12), 4262–4276. https://doi.org/10.1109/TITS.2018.2883766.
Zhou, Y., Kundu, T., Qin, W., Goh, M., Sheu, J.-B., 2021. Vulnerability of the worldwide air transportation network to global catastrophes such as COVID-19. Transp. Res. Part E: Logist. Transp. Rev. 154, 102469. https://doi.org/10.1016/j.tre.2021.102469.